Contents lists available at ScienceDirect

Computational Biology and Chemistry

journal homepage: www.elsevier.com/locate/cbac





Decoding the role of novel long noncoding RNAs lnc-SLC6A12-1:3 and lnc-SLC6A12-7:5 in regulating the expression of *GAD1* and *SLC6A12* in cholangiocarcinoma

Sharma Manjunath Arun, Neerkaje Subrayabhat Devaki *,1

Department of Molecular Biology, Yuvaraja's College, University of Mysore, Mysuru, Karnataka 570005, India

ARTICLE INFO

Keywords: LncRNA Cholangiocarcinoma SLC6A12 GAD1 Lnc-SLC6A12-1:3 Lnc-SLC6A12-7:5

ABSTRACT

Cholangiocarcinoma (CCA) is an aggressive bile duct malignancy with a poor prognosis and limited treatment options. Recent studies highlight the role of metabolic and signalling pathways in tumour progression and resistance, including neurotransmitter-related pathways like gamma-aminobutyric acid (GABA). Key GABAassociated genes, such as Solute Carrier Family 6 Member 12 (SLC6A12), a GABA transporter and Glutamate Decarboxylase 1 (GAD1) involved in GABA synthesis, are implicated in cancer but remain poorly understood in CCA. This study aims to identify novel long non-coding RNAs (lncRNAs) specifically associated with cholangiocarcinoma (CCA) and to explore their potential mechanisms of action. By integrating transcriptomic data and interaction prediction tools, we focus on lncRNAs that are linked to key differentially expressed metabolic genes, thereby uncovering their possible roles in the metabolic reprogramming of CCA. Using RNA-Seq data from the Sequence Read Archive (SRA), differential expression analysis identified 84 differentially expressed metabolic genes (DEMGs) associated with metabolic pathways. Gene ontology and pathway analyses using DAVID and Reactome database revealed pathway enrichment due to DEGs, while protein interaction using STRING, functionally connected SLC6A12/BGT1 and GAD1/GAD67. Two novel downregulated long non-coding RNAs (lncRNAs), lnc-SLC6A12-1:3 and lnc-SLC6A12-7:5, were identified based on expression correlations and genomic proximity to SLC6A12 and GAD1 genes. Interaction predictions using IntaRNA and lncTAR tools suggested lncRNA-mRNA interactions between the lncRNAs and mRNAs (SLC6A12 and GAD1). Transcription factor (TF) enrichment analysis using the CiiiDER tool and RNA-protein interaction predictions with the catRAPID tool revealed lnc-SLC6A12-1:3 functions as a regulatory scaffold, influencing the transcription of SLC6A12 and GAD1 by recruiting TFs such as IRF1, THAP1, FOSL1, and NR4A1. Whereas lnc-SLC6A12-7:5 did not show strong binding to TFs. In Ideal conditions, Inc-SLC6A12-1:3 enhances SLC6A12 expression by promoting IRF1 and FOSL1 activity but antagonises THAP1 and NR4A1, leading to the checked expression of GAD1. These interactions highlight a complex regulatory network where lnc-SLC6A12-1:3 and lnc-SLC6A12-7:5 differentially modulate transcription factor activity, balancing the expression of these key genes in CCA. For the first time, this in silico study reveals that two novel long non-coding RNAs, lnc-SLC6A12-1:3 and lnc-SLC6A12-7:5, regulate the expression of SLC6A12 and GAD1 through cis and trans binding interactions, respectively. Based on these interactions, we hypothesise that these lncRNAs may contribute to the modulation of the GABAergic pathway, which plays a crucial role in fulfilling the high energy demands of cholangiocarcinoma cells. Further experimental validation and investigation into the regulation of SLC6A12 and GAD1 are required to gain deeper insights into CCA pathogenesis and to identify potential therapeutic targets.

1. Introduction

Cholangiocarcinoma (CCA) is an aggressive malignancy originating

from the biliary epithelium, constitutes 15% of primary liver cancers and 3% of gastrointestinal malignancies (Elgenidy et al., 2022). CCA is classified anatomically into intrahepatic (iCCA), perihilar (pCCA), and

^{*} Correspondence to: Department of Molecular Biology, Yuvaraja's College, University of Mysore, Mysuru 570005, India. *E-mail addresses:* lionelarun@gmail.com (S.M. Arun), nsdevaki@ycm.uni-mysore.ac.in (N.S. Devaki).

¹ **Orcid ID:** 0000–0003-1360–9360

distal (dCCA) subtypes. While pCCA is the most prevalent, accounting for 50-60 % of CCAs. It is the second most common primary liver cancer after hepatocellular carcinoma. In the United States, bile duct cancer is relatively rare, with about 8000 new cases diagnosed annually (Statistics About Bile Duct Cancer | Cholangiocarcinoma Stats | American Cancer Society, n.d.). The incidence of CCA has been increasing globally, with notable rises in both intrahepatic and extrahepatic forms (Patel, 2002). However, the actual number may be higher due to diagnostic challenges. Mortality rates have also shown an upward trend; for instance, in Europe, the age-standardised mortality rate rose from 2.6 per 100,000 in 2001-4.7 per 100,000 in 2017 (Genus et al., 2019). Despite advancements in medical science, the prognosis for CCA remains poor, with a five-year survival rate of less than 10 % for most patients (Elgenidy et al., 2022). The global incidence and mortality of CCA are increasing, with a 5-year survival rate of 7-20 % and poor outcomes due to late-stage diagnosis and limited therapeutic options. iCCA is highly aggressive and characterised by an abundant tumour microenvironment (Banales et al., 2020; Louis et al., 2020; Sulpice et al., 2013, 2016). This study aims to identify novel lncRNAs associated with CCA by focusing on those linked to differentially expressed metabolic genes. We further investigate their potential mechanisms of action, such as interactions with transcription factors and mRNAs, to provide insights into their regulatory roles in CCA progression.

Gamma-aminobutyric acid (GABA) is a key component of the tumour microenvironment, and it also plays a central role in the GABA shunt pathway in cancer. This pathway facilitates the conversion of α -ketoglutarate, generated in the TCA cycle, into succinate via the intermediates glutamate, GABA, and succinic semialdehyde (Balázs et al., 1970; Sarasa et al., 2020), with succinic semialdehyde being oxidised to succinate by succinic semialdehyde dehydrogenase (SSADH), which then re-enters the TCA cycle (Samborska et al., 2021; Struys et al., 2005). This GABA shunt pathway is utilised by cancer cells for its high energy requirement. When GABA is secreted into the extracellular space, it acts as a neurotransmitter in Neuron-Glia Interactions (Vélez-Fort et al., 2011), whereas in cancer, it is involved in tumour progression, invasion and immune evasion (Huang et al., 2022; Li et al., 2023). GABA synthesis is regulated by two isoforms of glutamate decarboxylase (GAD): GAD2/GAD65 and GAD1/GAD67. While GAD65 primarily facilitates GABAergic synaptic transmission and plasticity, GAD67 is responsible for metabolic GABA production (Lange et al., 2014; Li et al., 2023). GAT1, SLC6A13/GAT2, GAT3, and SLC6A12/BGT1 are involved in regulating GABA levels, with GAT1, SLC6A13, and GAT3 primarily responsible for GABA reuptake in the brain, while SLC6A12 not only participates in GABA transport but also helps maintain osmotic balance and regulates betaine levels in the brain, kidney, and liver highlighting its broader roles (Bhatt et al., 2023; Kempson et al., 2014). Glutamate decarboxylase 1 (GAD1) is an enzyme that catalyses the conversion of glutamate to GABA. GAD activity is increased in certain types of human tumours such as colon, gastric, ovarian, and breast cancers (Young and Bordey, 2009). Studies have linked the GABAergic system to neoplastic processes, with increased GABA content and GAD activity observed in colon and breast cancer tissues. In a study, GABA content and GAD activity were significantly elevated in neoplastic tissue compared to the unaffected stomach tissue (Matuszek et al., 2001). Increased GABA levels and GAD activity were found in human colon cancer tissue compared to normal colon tissue from the same patients. Comparable findings were observed in athymic mice transplanted with human colon adenocarcinoma cells, where increased levels of GABA and GAD activity were detected in growing tumours compared to unaffected tissues. Notably, GAD activity was also markedly higher in the unaffected colon tissue adjacent to tumours in tumour-bearing mice compared to healthy control mice, while GABA levels were normal in the skin tissue, which is away from the tumour of experimental mice. These findings suggest that altered GABA metabolism may reflect a local immune response to cancer, and targeting the GABAergic system could offer therapeutic potential (Kleinrok et al., 1998). Elevated GABA levels and GAD activity in tumour tissue compared to normal mammary tissue in both humans and mice, with a positive correlation between the two. This increase may indicate a local immune response or tumour hypoxia (Mazurkiewicz et al., 1999). Many differentially expressed genes (DEGs) related to the tumour microenvironment (TME) were identified, primarily enriched in immune-related processes and pathways. Among these, *GAD1* was developed to predict cholangiocarcinoma (CCA) prognosis (Cao et al., 2021). Although direct evidence of GABA in CCA is scarce, the involvement of *GAD1* and *SLC6A12* in GABA synthesis suggests a potential role in modulating the tumour microenvironment and involvement of GABA in the GABA shunt pathway for increased energy demands in CCA.

Investigating the regulation of GAD1 and the SLC6A12 in CCA could uncover potential novel therapeutic targets, highlighting the critical role of the GABAergic system in cancer progression. Although no known interactions have been reported involving the long non-coding RNAs (lnc-SLC6A12–1:3 and lnc-SLC6A12–7:5), which regulate the genes involved in GABA synthesis (GAD1) and GABA transport (SLC6A12), this study seeks to establish a potential link among them by focusing on both lncRNA-mRNA interaction and lncRNA-protein interaction.

2. Materials and methods

2.1. Retrieval and processing of RNA-seq data

To investigate novel lncRNAs in Cholangiocarcinoma (CCA) patients, the dataset comprising 18 samples from adjacent non-tumour/normal liver tissues and 16 tumour samples was retrieved from SRP159264 available in the Sequence Read Archive (SRA) database (Katz et al., 2022).

Raw RNA-Seq data were downloaded as Fastq files using the function "fastq-dump- split-files". Quality check was assessed using FastQC. HISAT2 aligner was used to trim and align the reads to the human hg38 reference genome (Andrews, 2010). and were further compressed, sorted, and indexed using SAMtools (Desai et al., 2022; Kumari et al., 2021). The "flagstat" function within SAMtools was used to evaluate the quality of aligned files. The "coveragebed" function from the BEDTools suite was used to obtain the data matrix file (Quinlan and Hall, 2010). The BED file containing long non-coding RNA (lncRNA) and mRNA data was obtained from the LNCipedia database and UCSC Table Browser, respectively (Karolchik et al., 2004; Volders et al., 2013). To analyse the differential expression of the global transcriptome, we performed statistical evaluations on the read count files using the DESeq2 package in RStudio (Love et al., 2014). Additionally, the read counts were normalised to transcripts per million (TPM) to ensure comparability across samples and improve the accuracy of downstream analyses (Fig. 1). Validation was performed using the TCGA-CHOL dataset, which includes 9 normal and 35 primary tumour patient samples.

2.2. Global transcriptome analysis using DeSeq2 and metabolic pathway filtering

For a comprehensive understanding of the differential expression of the global transcriptome, we applied statistical analysis using the DESeq2 package to the read counts files (Love et al., 2014). The results from DESeq2 were integrated with the TPM data frame using gene symbols as the common key. To compute fold change (FC) for each tumour sample, the TPM value of the tumour samples was divided by the geometric mean of TPM values from normal samples. The resulting FC values were then log2 transformed to derive log2 fold change (l2fc) values. To shortlist mRNAs, we utilised 748 metabolic functional gene annotations from the nCounter® Metabolic Pathways Panel. This panel encompasses key pathways and processes essential for defining cellular metabolism. These 748 genes are then further filtered, where statistically significant mRNAs were filtered based on the DESeq2 data and mRNAs with a p-value greater than 0.05 were excluded. Differentially

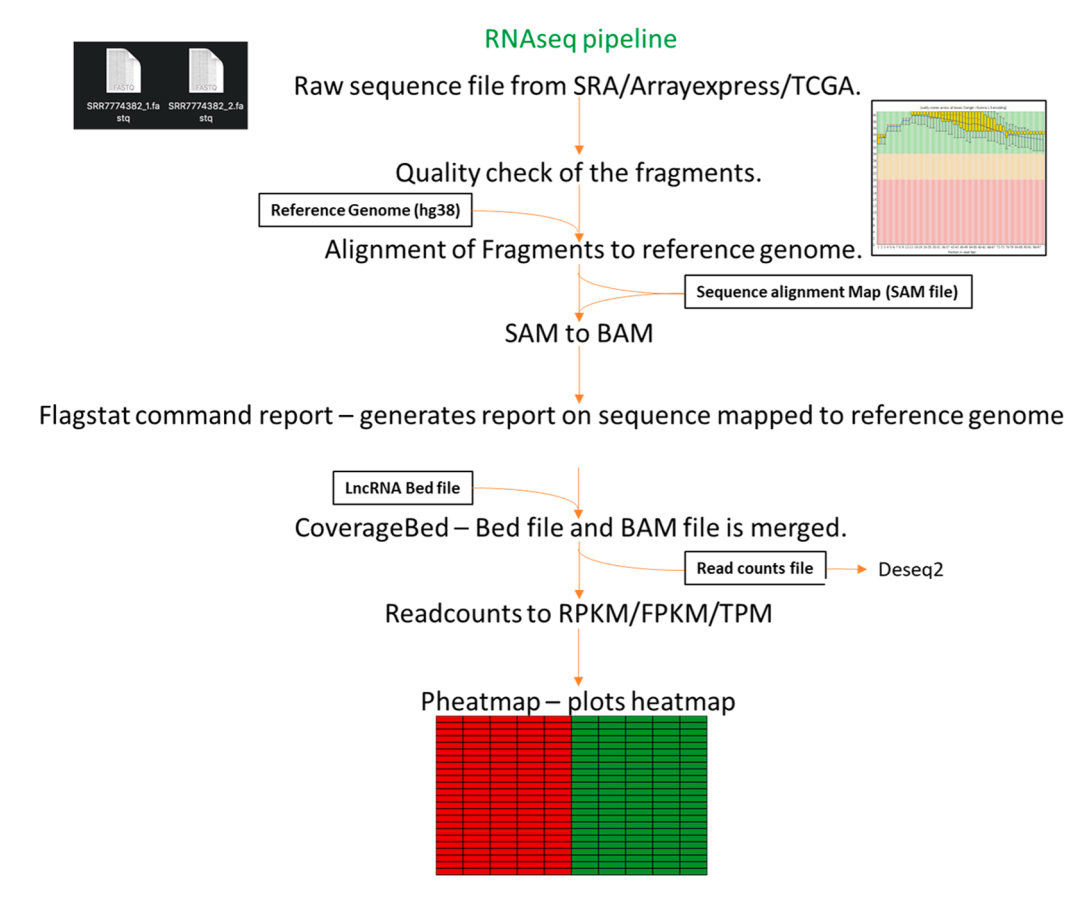


Fig. 1. RNA-Seq pipeline for analysing differential expression of both lncRNA and mRNA. The schematic outlines the RNA-seq pipeline beginning with quality control using FastQC, followed by trimming and alignment of the reads to the reference genome with HISAT2. Read counts are then quantified using feature Counts with Samtools and BEDtools. Finally, TPM is used for expression level comparison, and DESeq2 for normalisation and differential expression analysis. The data is then analysed and visualised using different statistical and graphical outputs.

expressed metabolic genes (DEMGs) were identified based on l2fc thresholds, greater than 2 or less than -2, for each tumour sample. Detailed computational and statistical protocols are available in the accompanying R script (Supplementary file 1)

2.3. Functional enrichment and pathway analysis using DAVID and reactome databases

The identified gene list was analysed using the DAVID database by employing the "Functional Annotation Clustering" function with default parameters (Dennis et al., 2003). The output was saved in a TSV format and imported into R using "read.csv". R libraries such as ggplot2, dplyr, and ggrepel were utilised for data processing and visualisation. The results were sorted by false discovery rate (FDR). From the ranked data, the top 10 entries were selected, focusing on Gene Ontology (GO) annotations, including GO Biological Processes (GO BP), Cellular Components (GO CC), and Molecular Functions (GO MF). The Reactome Database was used to get the metabolic pathway Annotations, and the default parameters were used (Milacic et al., 2024). These annotations were visualised in a bubble plot generated using ggplot2, which displayed the relationship between rank, -log10(FDR), gene size, and process labels. This visualisation provided an intuitive overview of the enriched functional categories and their statistical significance, aiding in the interpretation of the underlying biological processes.

2.4. Screening differentially expressed lncRNAs based on genomic Loci and expression pattern correlation

LncRNAs were considered relevant and shortlisted if they were

located within the same genomic region as the shortlisted mRNAs of interest by showing a significant positive or negative correlation with p-value < 0.05 and an L2FC greater than 2 or less than -2. This comprehensive approach enhances the accuracy of identifying differentially expressed lncRNAs that may have functional roles related to the regulation of protein-coding genes. Detailed steps can be found in the R script provided as Supplementary file 1.

2.5. lncRNA-mRNA interaction

RNA-RNA interactions were predicted using IntaRNA (version 2.0) with default parameters (Mann et al., 2017). The RNA sequences were retrieved from the UCSC Genome Browser and LNCipedia. IntaRNA was locally installed and used to predict RNA-RNA interactions between lncSLC6A12_1 and SLC6A12 mRNA using minimum free energy (MFE)-based modelling. The analysis was performed with –mode=M, specifying mRNA as the target (-t mRNA.fa) and lncRNA as the query (-q lncRNA.fa), enforcing a minimum base-pairing constraint of four consecutive nucleotides (–seedBP=4). Output files (tMinE, qMinE, and pMinE) were generated to extract minimum energy profiles and identify high-confidence binding regions, which were further analysed using custom R scripts for Heatmap visualisation. As validation, lncTAR was applied to the IntaRNA-identified lncRNA-mRNA regions, using a normalised ΔG cutoff of zero to confirm interactions.

2.6. lncRNA-protein interaction

To identify enriched transcription factors, the CiiiDER tool was used, DEMGs serving as the gene set, while non-differentially expressed

mRNAs with a log2 fold change (L2FC) between -0.4 and 0.4 were used as the background. This approach enabled the identification of the topenriched transcription factor (Gearing et al., 2019). Additionally, catRAPID was utilised to analyse lncRNA-transcription factor interactions. Protein FASTA sequences were retrieved from UniProt, while lncRNA sequences were obtained from LNCipedia. catRAPID was executed with default parameters, and the top-ranking interactions between lncRNAs and transcription factors were identified (Armaos et al., 2021).

2.7. Gene interaction prediction and network visualisation using STRING database

The STRING (Search Tool for the Retrieval of Interacting Genes/Proteins) database was utilised to predict interactions among the shortlisted genes and visualise their complex networks. For the analysis, we used the DEMGs as input and the Markov Cluster Algorithm as a scalable unsupervised clustering algorithm for the network graphs with an interaction score threshold of > 0.4 (Franceschini et al., 2013).

3. Results

3.1. Screening and differential expression analysis of metabolic genes in tumour samples

748 Metabolic functional gene annotations from the nCounter® Metabolic Pathways Panel, encompassing core pathways and processes critical to cellular metabolism, were utilised to shortlist mRNAs. These mRNAs are then filtered based on P-value (< 0.05) where 494 mRNAs are found to be significantly expressed (Fig. 2a). The subsequent level 2 filter revealed "41" mRNAs overexpressed with L2FC values greater than 2 and "43" mRNAs downregulated with L2FC less than -2 across all analysed tumour samples, accounting to 84 differentially expressed

metabolic genes (DEMGs) (Fig. 2b).

3.2. Pathway analysis and functional categorisation of differentially genes

The DEMGs were categorised based on their roles in cellular metabolism as annotated by the nCounter® Metabolic Pathways Panel. Upregulated genes are distributed across 22 cellular metabolic pathways (CMPs), while downregulated genes are associated with 17 pathways. Among these, 11 pathways contain both overexpressed and downregulated genes (Fig. 3a). The top 10 enriched CMPs include Autophagy, Cytokine & Chemokine Signalling, Fatty Acid Synthesis, Cell Type, PI3K, Nucleotide Salvage, NF-κB, Amino Acid Transporters, Glutamine Metabolism, and the Pentose Phosphate Pathway, with the percentage of genes involved ranging from 6.9 % to 30.7 % (Table 1). Conversely, the top 10 pathways with downregulated genes include Epigenetic Regulation, Transcriptional Regulation, AMPK, Glutamine Metabolism, Antigen Presentation, Tryptophan/Kynurenine Metabolism, Glucose Transport, Internal Reference, Amino Acid Synthesis, and PI3K, with the percentage of genes involved ranging from 5.2 % to 41.6 % (Table 2). Among these, the PI3K and Glutamine Metabolism pathways exhibit both overexpressed and downregulated genes. In the PI3K pathway, 10.5 % of the genes are upregulated, while 5.2 % are downregulated. Similarly, 7.5 % of the genes are upregulated in the Glutamine Metabolic pathway, whereas 22.5 % are downregulated, indicating a nuanced regulation of these pathways (Tables 1-2).

Network analysis was conducted using the DAVID and Reactome databases, with all 84 DEMGs provided as input under default parameters. In DAVID, only the enrichment of Gene Ontology (GO) annotation terms was considered. From the results of both DAVID and Reactome, the top 10 pathways meeting the criteria of at least three gene counts per pathway and FDR < 0.05 were selected and bubble plots were plotted, where the x-axis represents the rank of pathways based on enrichment

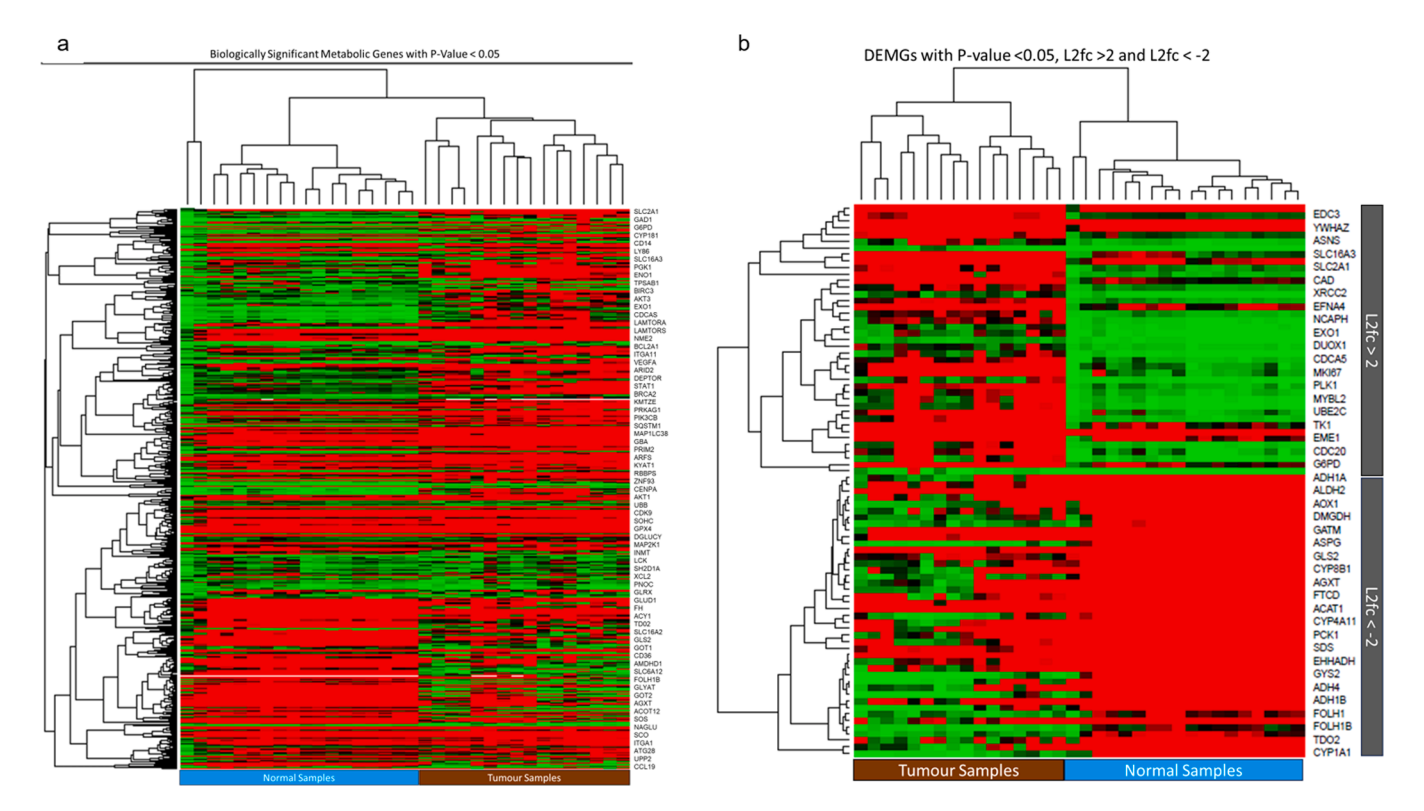


Fig. 2. Metabolic pathway genes expression pattern using TPM normalised data. Heatmap Comparison of genes represented as Metabolic pathway genes with filtering based on parameters as defined below. a. Heatmap showing the expression of mRNAs with a p-value less than 0.05. b. Heatmap showing the expression of mRNAs, focusing only on those with a p-value less than 0.05 and l2fc greater than 2 and l2fc less than -2 (Green denotes low expression and Red denotes high expression).

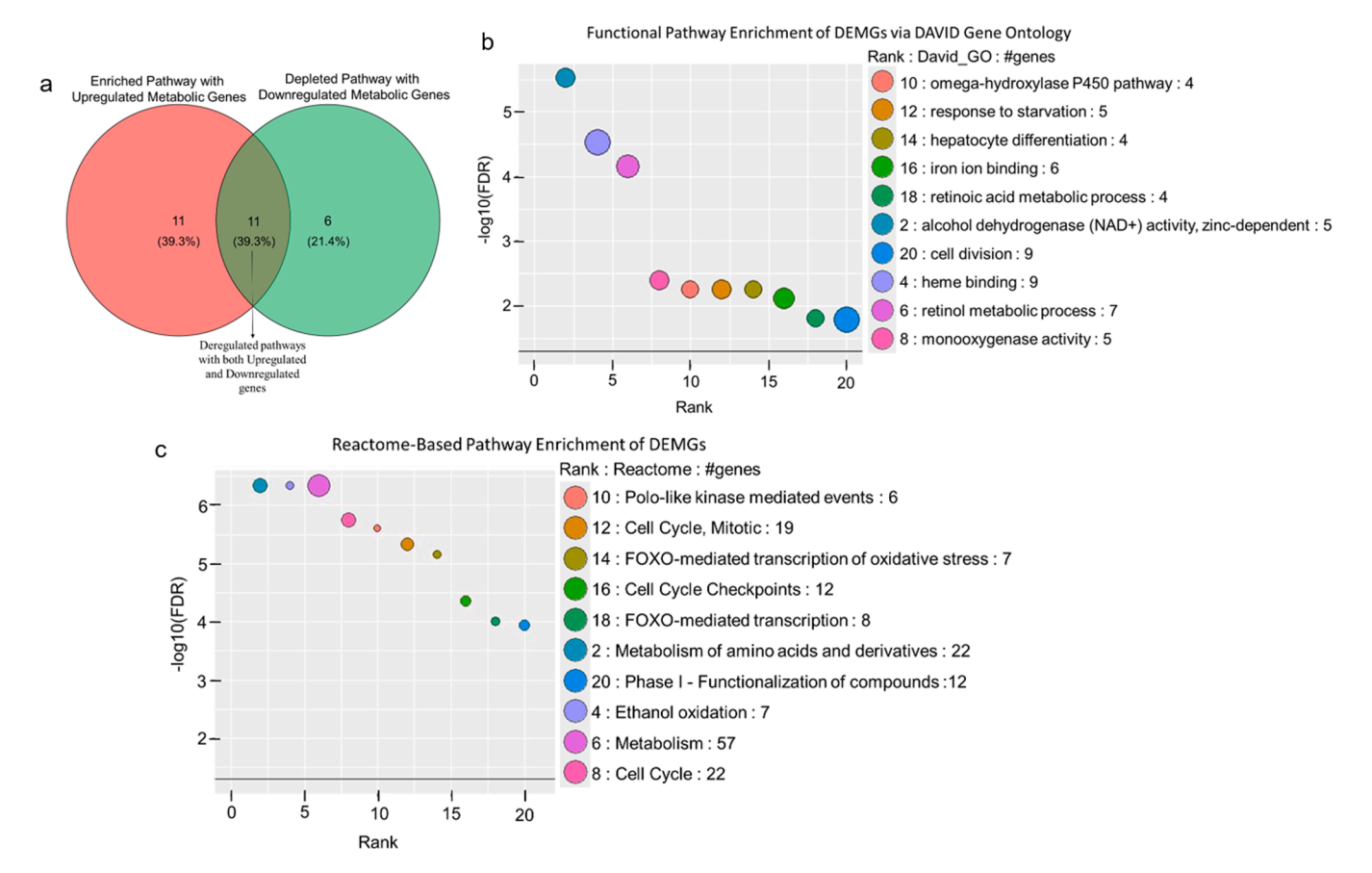


Fig. 3. Deregulated and enriched pathways. a. Venn diagram illustrating the distribution of upregulated, downregulated, and pathways containing both upregulated and downregulated genes in CCA. b & c. Bubble plots representing pathway enrichment analysis of DEGs using DAVID and Reactome databases. "Count" denotes the number of DEGs enriched in each pathway. The X-axis represents the rank, indicating the number of deregulated genes representing the pathway, while the Y-axis shows the -log10(FDR). The number of genes representing deregulated genes is denoted by "#genes". The top 10-ranked pathways are depicted in the plot.

significance, and the y-axis displays the -log10(FDR), indicating the statistical significance of the pathways. Each bubble corresponds to a specific pathway, with the legend showing the rank, pathway name, and associated gene count (Fig. 3b-c).

The most significant GO terms include the heme binding, alcohol dehydrogenase (NAD⁺Activity and retinol metabolic process. Mid-range significant pathways include monooxygenase activity, omegahydroxylase P450 pathway, response to starvation, hepatocyte differentiation and iron ion binding. Lower-ranked yet statistically relevant pathways include the retinoic acid metabolic processes and cell division. Cell division and heme binding pathways each involve 9 genes, making them the GO terms with the highest gene representation (Fig. 3 b).

Metabolism emerges as the most enriched pathway using the Reactome database, involving 57 genes, followed by metabolism of amino acids and derivatives and cell cycle, with 22 genes each ranking 1st and 4th based on FDR value, ethanol oxidation ranks 2nd with 9 genes. Pololike kinase-mediated events, mitotic cell cycle, and FOXO-mediated transcription of oxidative stress show Mid-range significance involvement, which can be grouped under cell division and stress responses. Other pathways, including "Phase I - Functionalization of compounds, cell cycle checkpoints and FOXO-mediated transcription," emphasise the role of metabolic and regulatory and cell cycle pathways (Fig. 3c).

3.3. Differential expression of LncRNAs in tumour and normal samples

LncRNAs are non-coding RNAs longer than 200 nucleotides. LncRNAs transcribed from the same loci as deregulated mRNAs were included, identifying 441 lncRNAs, including lncRNA isoforms and variants, corresponding to 84 deregulated genes. Among these 441

lncRNAs, 200 were statistically significant, with a p-value less than 0.05 (Fig. 4a). None of these 200 lncRNAs were upregulated with a log2 fold change (l2fc) greater than 2 but 34 lncRNAs were downregulated l2fc < -2 (Fig. 4b). However, 18 lncRNAs were downregulated with an l2fc less than -2, and showed a transcript per million (TPM) value below 0.8 across all tumour samples (Fig. 4c). Among these 18 lncRNAs, two novel lncRNAs (lnc-SLC6A12-1:3 and lnc-SLC6A12-7:5) were expressed with a TPM value greater than 0.7 in all normal samples (Fig. 4d). These lncRNAs are intronic lncRNAs which are located within the locus of gene *SLC6A12*. And could be involved in the regulation of the gene by the cisacting function of the lncRNA (Gil and Ulitsky, 2019). To confirm this, we performed an lncRNA-mRNA interaction study using the IntaRNA tool.

3.4. Functional insights into lncRNA-mRNA interactions: stability and binding dynamics

Inc-SLC6A12–1:3 is transcribed from the locus overlapping with *SLC6A12* and lnc-SLC6A12–7:5 corresponding *SLC6A13* locus adjacent to *SLC6A12* on the genome (Fig. S1a-S1c). The analysis of lncRNA-mRNA interactions highlights the functional roles of lncRNAs, which either suppress gene expression or enhance gene stability. IntaRNA analysis revealed distinct minimum interaction energies among the lncRNA-mRNA pairs. The pair lnc-SLC6A12–1:3 and *SLC6A12* exhibited the lowest interaction energy of –44.34 kcal/mol, indicating the highest interaction, occurring between nucleotides 283–409 of lnc-SLC6A12–1:3 and 2526–2665 of *SLC6A12*, signifying a thermodynamically favourable and stable binding (Figs. 5a, 5g & S2a). Conversely, the pair lnc-SLC6A12–7:5 and *SLC6A12* displayed an interaction energy of

Table 1

Top Enriched Pathways with Upregulated Genes in CCA. The table presents the top enriched pathways based on upregulated genes in cholangiocarcinoma (CCA). Columns include the pathway name, the total number of genes in the pathway (Total_Gene_Count_in_Pathway), the number of upregulated genes (Upr_Gene_Count) and the percentage of upregulated genes within each pathway. Pathways such as autophagy, cytokine & chemokine signaling, and fatty acid synthesis exhibit the highest proportion of upregulated genes, highlighting their potential role in CCA progression.

Unique_Pathway	Total_Gene_Count_in_Pathway_	Genes_Under_Pathway	Upr_Gene_Count	Upr_Genes_Under_Pathway	Percentage
Autophagy	65	ABL1,BRCA1,BRCA2,BRCC3,BRIP1, BUB1,BUB1B,CCNB2,CDCA5,CDCA8, CENPA,CLSPN,EXO1,FOXM1,GSK3B, GTSE1,HJURP,HSPA2,JAK2,MK167, MYBL2,MYC,NCAPH,NDC1,NPM1, NUP205,NUP62,PLK1,POLE,PRIM1, PRIM2,PTK6,RAD51,RANBP2,RRM2, SEM1,SMAD2,SMAD3,SMAD4,TK1, TP53,TPR,TYMS,WRN,YWHAZ, CCNA1,CCNA2,CCND1,CDC20, KIF2C,MAPK1,PSMA3,PSMA7, PSMB1,PSMB10,PSMB3,PSMC1, PSMD13,PSME2,SEC13,UBB,UBE2C, AKT1,AKT2,AKT3	20	BUB1B,CCNB2,CDCA5,CDCA8, CENPA,CLSPN,EXO1,FOXM1,GTSE1, MKI67,MYBL2,NCAPH,PLK1,PRIM2, SMAD3,TK1,YWHAZ,CDC20,KIF2C, UBE2C	30.76923077
Cytokine & Chemokine Signaling	31	COPS6,DTL,EME1,ERCC6,FANCA, FANCD2,FANCI,GPS1,MSH2,PCLAF, RAD51AP1,TIMELESS,UBE2T, XRCC2,ABL1,BRCA1,BRCA2,BRCC3, BRIP1,CLSPN,EXO1,KPNA2,POLE, POLR2A,RAD51,WRN,CCNA1, CCNA2,MAPK8,TP53,UBB	6	EME1,FANCD2,MSH2,XRCC2,CLSPN EXO1	, 19.35483871
Fatty Acid Synthesis	6	SLC2A1,SLC2A14,SLC2A3,SLC2A5, SLC2A6,SLC2A8	1	SLC2A1	16.66666667
Cell Type	20	ABCF1,AGK,COG7,DHX16,DNAJC14, EDC3,FCF1,G6PD,MRPS5,NRDE2, OAZ1,POLR2A,SAP130,SDHA, STK11IP,TBC1D10B,TBP,TLK2,UBB, USP39	3	EDC3,G6PD,TBC1D10B	15
PI3K	19	DERA,H6PD,IDNK,PGD,RBKS,RGN, RPIA,TKT,ALDOA,ALDOB,GLYCTK, PRPS1,TALDO1,FBP1,G6PD,GPI, PFKL,PFKM,PGM2	2	ALDOA,G6PD	10.52631579
Nucleotide Salvage	49	AK3,CDK9,CTPS1,GART,GDA,GMPS, IMPDH1,IMPDH2,NPR1,NPR2,NT5E, PRPS1,RRM1,UMPS,XDH,ADA,ADK, AMPD1,AMPD2,AMPD3,APRT,CDA, DCK,DGUOK,GMPR,GMPR2,HPRT1, NME1,NME2,PGM2,PKLR,PKM,PNP, PRIM1,PRIM2,RRM2,TK2,TYMP, TYMS,UCK1,UCK2,UCK11,UPP1, UPP2,CAD,POLE,POLR2A,PPAT,TK1	5	PKM,PRIM2,UCK2,CAD,TK1	10.20408163
NF-KB	23	ADA,ADAL,ADK,AMPD1,AMPD2, AMPD3,APRT,CDA,DCK,DGUOK, GMPR,GMPR2,HPRT1,PNP,PUDP, TK2,TYMP,UCK1,UCK2,UCKL1, UPP1,UPP2,TK1	2	UCK2,TK1	8.695652174
Amino Acid Transporters	36	AP2S1,BTK,CD14,CDC20,CTSA, CTSD,CTSL,CTSS,CYBB,HERC1,HLA- A,HLA-C,HLA-DQA1,HLA-DRB1,HLA- E,ITCH,ITGB5,KEAP1,KIF2C,LAG3, LY96,MYD88,PSMA3,PSMA7,PSMB1, PSMB10,PSMB3,PSMC1,PSMD13, PSME2,SEC13,TLR2,TLR4,UBE2C, VHL,CD36	3	CDC20,KIF2C,UBE2C	8.33333333
Glutamine Metabolism	40	ALDOA,ALDOB,ENO1,ENO3,GAPDH, GAPDHS,GCK,GPI,HK1,HK2,HK3, PDHA1,PGK1,PGM2,PKLR,PKM, FBP1,G6PC,LDHA,LDHB,LDHC,PCK1, PCK2,PFKFB1,PFKL,PFKM,PGAM2, ADH1A,ADH1B,ADH1C,ADH4,ADH6, ADH7,ALDH2,NDC1,NUP205,NUP62, RANBP2,SEC13,TPR	3	ALDOA,GAPDH,PKM	7.5
Pentose Phosphate Pathway	43	APOE,ATOX1,CA12,CAT,DUOX1, DUOX2,GPX1,GPX4,KRT1,MPO, MSRB2,MTF1,NOX1,NOX3,NOX4, PEBP1,PRDX5,PRKN,PTGS1, SELENOK,SOD3,TXN2,ERCC6,FDX1, FDXR,GCLC,IDH1,NDUFA12, NDUFA6,NDUFB4,NDUFS8,NQO1, PRDX1,SLC7A11,SOD1,ABL1,BCL2,	3	DUOX1,NOX1,NOX4	6.976744186
				(co	ontinued on next page

(continued on next page)

Table 1 (continued)

Unique_Pathway	Total_Gene_Count_in_Pathway_	Genes_Under_Pathway	Upr_Gene_Count	Upr_Genes_Under_Pathway	Percentage
		EGFR,JAK2,AKT1,HMOX1,PTGS2,			
·lvaolvoia	15	WRN	1	CA9	6.66666666
Glycolysis	15	CA9,HIF3A,SEM1,VEGFA,VHL, PSMA3,PSMA7,PSMB1,PSMB10,	1	CAY	0.000000007
		PSMB3,PSMC1,PSMD13,PSME2,UBB,			
(ucleotide	38	HIF1A PRDX1,TIGAR,TP63,TXN,TXNRD1,	2	G6PD, YWHAZ	5.263157895
Nucleotide Synthesis	36	COX14,COX4I1,COX5A,COX5B,	2	GOPD, I WHAZ	5.20315/695
		COX6A1,COX6B1,COX7B,COX7C,			
		COX8A,G6PD,GPI,NDUFA4,GLS,			
		GLS2,PRKAA1,RPTOR,MTOR, PRKAB1,PRKAG1,PRKAA2,PRKAB2,			
		PRKAG2,TP53,AKT1,AKT2,AKT3,			
		LAMTOR2,LAMTOR4,LAMTOR5,			
/litochondrial	20	MLST8,PTEN,RRAGC,YWHAZ HSPA4,HSPE1,NME1,NME2,RPL23,	1	CAD	5
Respiration	20	THBS1,CAD,ENO1,HERC1,NPM1,	1	CAD	3
1		ODC1,PPAT,SRM,TFRC,CCNA2,			
	00	LDHA,MYC,TP53,FASLG,FASN		GT CO.4.1	0.551.400551
ryptophan/ Kynurenine	28	AKR1C4,APOA1,APOA2,APOA4, APOC2,APOC3,APOM,CYP8B1,	1	SLC2A1	3.571428571
Metabolism		NADK,NADK2,RBP4,TTPA,TTR,			
		APOE,NT5E,SHMT1,SHMT2,SLC2A1,			
		SLC2A3,AOX1,FASN,NOS3,PTGS2,			
LR Signaling	59	AKT1,ACACA,ACACB,APOB,IDH1 AR,ASCL1,ATF7,EOMES,FOXP3,	2	FOXM1,MYBL2	3.389830508
		HSF1,HSF2,MYBL1,MYCL,MYCN,		,	
		NFAT5,NR2F1,RUNX1,RUNX2,SPIB,			
		SREBF2,TBX21,ZNF100,ZNF136, ZNF253,ZNF254,ZNF43,ZNF610,			
		ZNF675,ZNF682,ZNF708,ZNF85,			
		ZNF91,ZNF93,CLOCK,FOXM1,HIF3A,			
		HNF4A,IRF1,IRF4,MYB,MYBL2,			
		PPARG,REST,SOX2,SREBF1,STAT1, STAT3,STAT5A,STAT6,TBP,TP63,			
		HIF1A,MYC,NFKB2,TP53,NFKB1,			
		RELA,ATF4,CREB3L3,KMT2A,			
MPK	95	KMT2D,KMT2E,NFE2L2	3	ASNS,CAD,GAD1	3.157894737
VIPK	93	AADAT,ACAA2,ACAT1,ACAT2, ACSF3,ADH1A,ADH1B,ADH1C,	3	A3N3,CAD,GAD1	3.13/694/3
		ADH4,ADH6,ADH7,AGXT,AGXT2,			
		ALDH2,AMDHD1,AOC1,AOC3,AOX1,			
		ARG1,ASH1L,ASL,ASNS,ASPA,ASS1, BHMT,BHMT2,CAD,CPS1,DAO,DDC,			
		DMGDH,ECHS1,EHHADH,EZH2,FAH,			
		FAHD1,FOLH1,FTCD,GAD1,GATM,			
		GCDH,GCLC,GLS,GLS2,GLUD1,GLUL, GLYAT,GLYCTK,GOT1,GOT2,GPT,			
		HADH,HDC,HPD,IL4I1,KMT2A, KMT2D,KMT2E,KYAT1,KYAT3,			
		HADH,HDC,HPD,IL4I1,KMT2A, KMT2D,KMT2E,KYAT1,KYAT3, LDHA,LDHB,LDHC,LTA4H,MAT1A,			
		HADH,HDC,HPD,IL4I1,KMT2A, KMT2D,KMT2E,KYAT1,KYAT3, LDHA,LDHB,LDHC,LTA4H,MAT1A, MAT2A,NAT8L,NFS1,NOS1,NOS2,			
		HADH,HDC,HPD,IL4I1,KMT2A, KMT2D,KMT2E,KYAT1,KYAT3, LDHA,LDHB,LDHC,LTA4H,MAT1A,			
		HADH,HDC,HPD,IL4I1,KMT2A, KMT2D,KMT2E,KYAT1,KYAT3, LDHA,LDHB,LDHC,LTA4H,MAT1A, MAT2A,NAT8L,NFS1,NOS1,NOS2, NOS3,NSD1,OAT,ODC1,OGDH, OGDHL,PAH,PGAM2,PHGDH,PPAT, PRODH2,PSAT1,PSPH,PYCR1,			
		HADH,HDC,HPD,IL4I1,KMT2A, KMT2D,KMT2E,KYAT1,KYAT3, LDHA,LDHB,LDHC,LTA4H,MAT1A, MAT2A,NAT8L,NFS1,NOS1,NOS2, NOS3,NSD1,OAT,ODC1,OGDH, OGDHL,PAH,PGAM2,PHGDH,PPAT, PRODH2,PSAT1,PSPH,PYCR1, PYCR2,PYCR3,RIMKLA,RIMKLB,SDS,			
ucose Transport	35	HADH,HDC,HPD,IL4I1,KMT2A, KMT2D,KMT2E,KYAT1,KYAT3, LDHA,LDHB,LDHC,LTA4H,MAT1A, MAT2A,NAT8L,NFS1,NOS1,NOS2, NOS3,NSD1,OAT,ODC1,OGDH, OGDHL,PAH,PGAM2,PHGDH,PPAT, PRODH2,PSAT1,PSPH,PYCR1, PYCR2,PYCR3,RIMKLA,RIMKLB,SDS, SDSL,SHMT1,SHMT2,SRM,SRR,TH	1	ASNS	2 85714285
lucose Transport	35	HADH,HDC,HPD,IL4I1,KMT2A, KMT2D,KMT2E,KYAT1,KYAT3, LDHA,LDHB,LDHC,LTA4H,MAT1A, MAT2A,NAT8L,NFS1,NOS1,NOS2, NOS3,NSD1,OAT,ODC1,OGDH, OGDHL,PAH,PGAM2,PHGDH,PPAT, PRODH2,PSAT1,PSPH,PYCR1, PYCR2,PYCR3,RIMKLA,RIMKLB,SDS,	1	ASNS	2.85714285
lucose Transport	35	HADH,HDC,HPD,IL4I1,KMT2A, KMT2D,KMT2E,KYAT1,KYAT3, LDHA,LDHB,LDHC,LTA4H,MAT1A, MAT2A,NAT8L,NFS1,NOS1,NOS2, NOS3,NSD1,OAT,ODC1,OGDH, OGDHL,PAH,PGAM2,PHGDH,PPAT, PRODH2,PSAT1,PSPH,PYCR1, PYCR2,PYCR3,RIMKLA,RIMKLB,SDS, SDSL,SHMT1,SHMT2,SRM,SRR,TH ASPG,DGLUCY,FOLH1B,GADL1, GLRX,GRIN1,LTC4S,NAALAD2, PTGES,SERINC1,SERINC2,SERINC3,	1	ASNS	2.85714285
lucose Transport	35	HADH,HDC,HPD,IL4I1,KMT2A, KMT2D,KMT2E,KYAT1,KYAT3, LDHA,LDHB,LDHC,LTA4H,MAT1A, MAT2A,NAT8L,NFS1,NOS1,NOS2, NOS3,NSD1,OAT,ODC1,OGDH, OGDHL,PAH,PGAM2,PHGDH,PPAT, PRODH2,PSAT1,PSPH,PYCR1, PYCR2,PYCR3,RIMKLA,RIMKLB,SDS, SDSL,SHMT1,SHMT2,SRM,SRR,TH ASPG,DGLUCY,FOLH1B,GADL1, GLRX,GRIN1,LTC4S,NAALAD2, PTGES,SERINC1,SERINC2,SERINC3, SERINC5,ASNS,ASPA,FOLH1,KYAT1,	1	ASNS	2.857142857
lucose Transport	35	HADH,HDC,HPD,IL4I1,KMT2A, KMT2D,KMT2E,KYAT1,KYAT3, LDHA,LDHB,LDHC,LTA4H,MAT1A, MAT2A,NAT8L,NFS1,NOS1,NOS2, NOS3,NSD1,OAT,ODC1,OGDH, OGDHL,PAH,PGAM2,PHGDH,PPAT, PRODH2,PSAT1,PSPH,PYCR1, PYCR2,PYCR3,RIMKLA,RIMKLB,SDS, SDSL,SHMT1,SHMT2,SRM,SRR,TH ASPG,DGLUCY,FOLH1B,GADL1, GLRX,GRIN1,LTC4S,NAALAD2, PTGES,SERINC1,SERINC2,SERINC3, SERINC5,ASNS,ASPA,FOLH1,KYAT1, NAT8L,OAT,PHGDH,PSAT1,PSPH,	1	ASNS	2.857142857
lucose Transport	35	HADH,HDC,HPD,IL4I1,KMT2A, KMT2D,KMT2E,KYAT1,KYAT3, LDHA,LDHB,LDHC,LTA4H,MAT1A, MAT2A,NAT8L,NFS1,NOS1,NOS2, NOS3,NSD1,OAT,ODC1,OGDH, OGDHL,PAH,PGAM2,PHGDH,PPAT, PRODH2,PSAT1,PSPH,PYCR1, PYCR2,PYCR3,RIMKLA,RIMKLB,SDS, SDSL,SHMT1,SHMT2,SRM,SRR,TH ASPG,DGLUCY,FOLH1B,GADL1, GLRX,GRIN1,LTC4S,NAALAD2, PTGES,SERINC1,SERINC2,SERINC3, SERINC5,ASNS,ASPA,FOLH1,KYAT1,	1	ASNS	2.857142857
·		HADH,HDC,HPD,IL4I1,KMT2A, KMT2D,KMT2E,KYAT1,KYAT3, LDHA,LDHB,LDHC,LTA4H,MAT1A, MATZA,NATBL,NFS1,NOS1,NOS2, NOS3,NSD1,OAT,ODC1,OGDH, OGDHL,PAH,PGAM2,PHGDH,PPAT, PRODH2,PSAT1,PSPH,PYCR1, PYCR2,PYCR3,RIMKLA,RIMKLB,SDS, SDSL,SHMT1,SHMT2,SRM,SRR,TH ASPG,DGLUCY,FOLH1B,GADL1, GLRX,GRIN1,LTC4S,NAALAD2, PTGES,SERINC1,SERINC2,SERINC3, SERINC5,ASNS,ASPA,FOLH1,KYAT1, NATBL,OAT,PHGDH,PSAT1,PSPH, PYCR1,PYCR2,PYCR3,RIMKLA, RIMKLB,SRR,GLS,GLS2,GLUD1, GLUL,GOT1,GOT2,GPT			
NA Damage	35	HADH,HDC,HPD,IL4I1,KMT2A, KMT2D,KMT2E,KYAT1,KYAT3, LDHA,LDHB,LDHC,LTA4H,MAT1A, MAT2A,NAT8L,NFS1,NOS1,NOS2, NOS3,NSD1,OAT,ODC1,OGDH, OGDHL,PAH,PGAM2,PHGDH,PPAT, PRODH2,PSAT1,PSPH,PYCR1, PYCR2,PYCR3,RIMKLA,RIMKLB,SDS, SDSL,SHMT1,SHMT2,SRM,SRR,TH ASPG,DGLUCY,FOLH1B,GADL1, GLRX,GRIN1,LTC4S,NAALAD2, PTGES,SERINC1,SERINC2,SERINC3, SERINC5,ASNS,ASPA,FOLH1,KYAT1, NAT8L,OAT,PHGDH,PSAT1,PSPH, PYCR1,PYCR2,PYCR3,RIMKLA, RIMKLB,SRR,GLS,GLS2,GLUD1, GLUL,GOT1,GOT2,GPT ACAP2,APOB,ARF5,ARPC4,CD3D,	1	ASNS SMAD3	
·		HADH,HDC,HPD,IL4I1,KMT2A, KMT2D,KMT2E,KYAT1,KYAT3, LDHA,LDHB,LDHC,LTA4H,MAT1A, MATZA,NATBL,NFS1,NOS1,NOS2, NOS3,NSD1,OAT,ODC1,OGDH, OGDHL,PAH,PGAM2,PHGDH,PPAT, PRODH2,PSAT1,PSPH,PYCR1, PYCR2,PYCR3,RIMKLA,RIMKLB,SDS, SDSL,SHMT1,SHMT2,SRM,SRR,TH ASPG,DGLUCY,FOLH1B,GADL1, GLRX,GRIN1,LTC4S,NAALAD2, PTGES,SERINC1,SERINC2,SERINC3, SERINC5,ASNS,ASPA,FOLH1,KYAT1, NATBL,OAT,PHGDH,PSAT1,PSPH, PYCR1,PYCR2,PYCR3,RIMKLA, RIMKLB,SRR,GLS,GLS2,GLUD1, GLUL,GOT1,GOT2,GPT			
NA Damage		HADH,HDC,HPD,IL4I1,KMT2A, KMT2D,KMT2E,KYAT1,KYAT3, LDHA,LDHB,LDHC,LTA4H,MAT1A, MAT2A,NAT8L,NFS1,NOS1,NOS2, NOS3,NSD1,OAT,ODC1,OGDH, OGDHL,PAH,PGAM2,PHGDH,PPAT, PRODH2,PSAT1,PSPH,PYCR1, PYCR2,PYCR3,RIMKLA,RIMKLB,SDS, SDSL,SHMT1,SHMT2,SRM,SRR,TH ASPG,DGLUCY,FOLH1B,GADL1, GLRX,GRIN1,LTC4S,NAALAD2, PTGES,SERINC1,SERINC2,SERINC3, SERINC5,ASNS,ASPA,FOLH1,KYAT1, NAT8L,OAT,PHGDH,PSAT1,PSPH, PYCR1,PYCR2,PYCR3,RIMKLA, RIMKLB,SRR,GLS,GLS2,GUD1, GLUL,GOT1,GOT2,GPT ACAP2,APOB,ARF5,ARPC4,CD3D, CD3G,EEA1,FOLR1,FOLR3,GAPVD1,			
NA Damage		HADH,HDC,HPD,IL4I1,KMT2A, KMT2D,KMT2E,KYAT1,KYAT3, LDHA,LDHB,LDHC,LTA4H,MAT1A, MAT2A,NAT8L,NFS1,NOS1,NOS2, NOS3,NSD1,OAT,ODC1,OGDH, OGDHL,PAH,PGAM2,PHGDH,PPAT, PRODH2,PSAT1,PSPH,PYCR1, PYCR2,PYCR3,RIMKLA,RIMKLB,SDS, SDSL,SHMT1,SHMT2,SRM,SRR,TH ASPG,DGLUCY,FOLH1B,GADL1, GLRX,GRIN1,LTC4S,NAALAD2, PTGES,SERINC1,SERINC2,SERINC3, SERINC5,ASNS,ASPA,FOLH1,KYAT1, NAT8L,OAT,PHGDH,PSAT1,PSPH, PYCR1,PYCR2,PYCR3,RIMKLA, RIMKLB,SRR,GLS,GLS2,GLUD1, GLUL,GOT1,GOT2,GPT ACAP2,APOB,ARF5,ARPC4,CD3D, CD3G,EEA1,FOLR1,FOLR3,GAPVD1, NEDD8,PIK3C2A,SLC2A8,SNF8,TF, TFRC,USP8,VPS28,WASHC4,AP2S1, CBL,CD4,CHMP2A,CHMP6,COPS6,			
NA Damage		HADH,HDC,HPD,IL4I1,KMT2A, KMT2D,KMT2E,KYAT1,KYAT3, LDHA,LDHB,LDHC,LTA4H,MAT1A, MAT2A,NAT8L,NFS1,NOS1,NOS2, NOS3,NSD1,OAT,ODC1,OGDH, OGDHL,PAH,PGAM2,PHGDH,PPAT, PRODH2,PSAT1,PSPH,PYCR1, PYCR2,PYCR3,RIMKLA,RIMKLB,SDS, SDSL,SHMT1,SHMT2,SRM,SRR,TH ASPG,DGLUCY,FOLH1B,GADL1, GLRX,GRIN1,LTC4S,NAALAD2, PTGES,SERINC1,SERINC2,SERINC3, SERINC5,ASNS,ASPA,FOLH1,KYAT1, NAT8L,OAT,PHGDH,PSAT1,PSPH, PYCR1,PYCR2,PYCR3,RIMKLA, RIMKLB,SRR,GLS,GLS2,GLUD1, GLUL,GOT1,GOT2,GPT ACAP2,APOB,ARF5,ARPC4,CD3D, CD3G,EEA1,FOLR1,FOLR3,GAPVD1, NEDD8,PIK3C2A,SLC2A8,SNF8,TF, TFRC,USP8,VPS28,WASHC4,AP2S1, CBL,CD4,CHMP2A,CHMP6,COPS6, EGFR,GPS1,HSPA2,IL2RA,ITCH,			
) DNA Damage		HADH,HDC,HPD,IL4I1,KMT2A, KMT2D,KMT2E,KYAT1,KYAT3, LDHA,LDHB,LDHC,LTA4H,MAT1A, MAT2A,NAT8L,NFS1,NOS1,NOS2, NOS3,NSD1,OAT,ODC1,OGDH, OGDHL,PAH,PGAM2,PHGDH,PPAT, PRODH2,PSAT1,PSPH,PYCR1, PYCR2,PYCR3,RIMKLA,RIMKLB,SDS, SDSL,SHMT1,SHMT2,SRM,SRR,TH ASPG,DGLUCY,FOLH1B,GADL1, GLRX,GRIN1,LTC4S,NAALAD2, PTGES,SERINC1,SERINC2,SERINC3, SERINC5,ASNS,ASPA,FOLH1,KYAT1, NAT8L,OAT,PHGDH,PSAT1,PSPH, PYCR1,PYCR2,PYCR3,RIMKLA, RIMKLB,SRR,GLS,GLS2,GLUD1, GLUL,GOT1,GOT2,GPT ACAP2,APOB,ARF5,ARPC4,CD3D, CD3G,EEA1,FOLR1,FOLR3,GAPVD1, NEDD8,PIK3C2A,SLC2A8,SNF8,TF, TFRC,USP8,VPS28,WASHC4,AP2S1, CBL,CD4,CHMP2A,CHMP6,COPS6,			
Glucose Transport DNA Damage Repair		HADH,HDC,HPD,IL4I1,KMT2A, KMT2D,KMT2E,KYAT1,KYAT3, LDHA,LDHB,LDHC,LTA4H,MAT1A, MAT2A,NAT8L,NFS1,NOS1,NOS2, NOS3,NSD1,OAT,ODC1,OGDH, OGDHL,PAH,PGAM2,PHGDH,PPAT, PRODH2,PSAT1,PSPH,PYCR1, PYCR2,PYCR3,RIMKLA,RIMKLB,SDS, SDSL,SHMT1,SHMT2,SRM,SRR,TH ASPG,DGLUCY,FOLH1B,GADL1, GLRX,GRIN1,LTC4S,NAALAD2, PTGES,SERINC1,SERINC2,SERINC3, SERINC5,ASNS,ASPA,FOLH1,KYAT1, NAT8L,OAT,PHGDH,PSAT1,PSPH, PYCR1,PYCR2,PYCR3,RIMKLA, RIMKLB,SRR,GLS,GLS2,GLUD1, GLUL,GOT1,GOT2,GPT ACAP2,APOB,ARF5,ARPC4,CD3D, CD3G,EEA1,FOLR1,FOLR3,GAPVD1, NEDD8,PIK3C2A,SLC2A8,SNF8,TF, TFRC,USP8,VPS28,WASHC4,AP2S1, CBL,CD4,CHMP2A,CHMP6,COPS6, EGFR,GPS1,HSPA2,IL2RA,ITCH, SMAD2,STAM2,UBB,HLA-A,HLA-C, HLA-E,HRAS,SMAD3,TRAF6			2.857142857 2.564102564 2.409638554
DNA Damage Repair	39	HADH,HDC,HPD,IL4I1,KMT2A, KMT2D,KMT2E,KYAT1,KYAT3, LDHA,LDHB,LDHC,LTA4H,MAT1A, MAT2A,NAT8L,NFS1,NOS1,NOS2, NOS3,NSD1,OAT,ODC1,OGDH, OGDHL,PAH,PGAM2,PHGDH,PPAT, PRODH2,PSAT1,PSPH,PYCR1, PYCR2,PYCR3,RIMKLA,RIMKLB,SDS, SDSL,SHMT1,SHMT2,SRM,SRR,TH ASPG,DGLUCY,FOLH1B,GADL1, GLRX,GRIN1,LTC4S,NAALAD2, PTGES,SERINC1,SERINC2,SERINC3, SERINC5,ASNS,ASPA,FOLH1,KYAT1, NAT8L,OAT,PHGDH,PSAT1,PSPH, PYCR1,PYCR2,PYCR3,RIMKLA, RIMKLB,SRR,GLS,GLS2,GUD1, GLUL,GOT1,GOT2,GPT ACAP2,APOB,ARF5,ARPC4,CD3D, CD3G,EEA1,FOLR1,FOLR3,GAPVD1, NEDD8,PIK3C2A,SLC2A8,SNP8,TF, TFRC,USPB,VS28,WASHC4,AP2S1, CBL,CD4,CHMP2A,CHMP6,COPS6, EGFR,GPS1,HSPA2,LL2RA,ITCH, SMAD2,STAM2,UBB,HLA-A,HLA-C, HLA-E,HRAS,SMAD3,TRAF6	1	SMAD3	2.564102564

Table 1 (continued)

Unique_Pathway	Total_Gene_Count_in_Pathway_	Genes_Under_Pathway	Upr_Gene_Count	Upr_Genes_Under_Pathway	Percentage
		BAD,CMKLR1,CREB3L3,EFNA4, FGF1,GYS2,IL2,IL4,IL6,IL7,ITGB1,			
		ITGB5,PTK2,THBS1,TLR2,BCL2,			
		BCL2L1,EGFR,FASLG,GSK3B,INSR,			
		JAK2,MAP2K2,MLST8,PDPK1,PTEN,			
		RPS6KB1,RPS6KB2,SOS1,SOS2,			
		STK11, VEGFA, YWHAZ, CCND1,			
		KRAS,MAP2K1,MYC,NFKB1,NRAS, PIK3CA,PIK3CB,PIK3CD,PIK3R1,			
		PIK3R2,PIK3R3,PRKAA1,RELA,			
		RPTOR,HRAS,MAPK1,MTOR,			
		PRKAA2,TP53,AKT1,AKT2,AKT3,			
		BRCA1,CSF3R,FLT1,FLT3,G6PC,			
		GNG12,IL2RA,NGFR,NOS3,PCK1, PCK2,PDGFB,PDGFRB,TLR4			
mTOR	53	ATF4,CACNA1A,CACNA1E,CACNB4,	1	EFNA4	1.886792453
		CACNG2,CACNG3,CACNG7,			
		CMKLR1,EFNA4,FGF1,MAP3K12,			
		MAPK8IP1,MAPT,STK3,CD14,FASLG,			
		FLT1,FLT3,GNG12,MAP2K3,MRAS,			
		NGFR,PDGFB,PDGFRB,PPM1A, PRKCG,PTPN5,KRAS,MAP2K1,			
		MAPK8,NRAS,TP53,TRAF6,HRAS,			
		MAPK1,AKT1,AKT2,AKT3,BRAF,			
		EGFR,HSPA2,INSR,MAP2K2,MYC,			
		MYD88,NFKB1,NFKB2,RELA,			
Cell Cycle	124	RPS6KA1,SOS1,SOS2,TNF,VEGFA A2M,ALOX12,ALOX15,ALOX5,	2	SMAD3, YWHAZ	1.612903226
Cen Cycle	124	BIRC3,BRAF,CBL,CCL13,CCL19,	2	SWADS, I WHAL	1.012903220
		CCL4,CCL5,CD27,CD4,CD40LG,			
		CSF3R,CXCL9,CXCR6,EGFR,FASLG,			
		FLT1,FLT3,FPR1,GNG12,HMOX1,			
		IFNG,IL10,IL2,IL21R,IL2RA,IL4,IL6, IL7,IRF1,IRF4,ITGAM,ITGB1,ITGB2,			
		ITK,KPNA2,LCK,LTA,LTB,MAP2K3,			
		NFKB1,NFKB2,NGFR,NOD2,PDGFB,			
		PDGFRB,PLCG1,PTGS2,PTK2,PTPN5,			
		RELA,RPLPO,RPS6KA1,S100A12,			
		SOD1,SOD2,SOS1,SOS2,SOX2, SQSTM1,STAM2,STAT1,STAT3,			
		STAT5A,STAT6,TALDO1,TBK1,TNF,			
		TNFRSF17,TNFRSF4,VEGFA,AOX1,			
		BCL2,BCL2L1,GSK3B,HIF1A,HLA-A,			
		HLA-C,HLA-DQA1,HLA-DRB1,HLA-E,			
		HRAS, JAK2, KRAS, LEPR, MAP2K1,			
		MAPK8,MYC,MYD88,NDC1,NRAS, NUP205,NUP62,RANBP2,SMAD3,			
		TP53,TPR,TRAF6,YWHAZ,AKT1,			
		AKT2,AKT3,CCND1,CD36,MAPK1,			
		MTOR,NOS2,PIK3CA,PIK3CB,			
		PIK3CD,PIK3R1,PIK3R2,PIK3R3,			
		PSMA3,PSMA7,PSMB1,PSMB10, PSMB3,PSMC1,PSMD13,PSME2			
MAPK	74	ATP5F1D,ATP5ME,COX14,COX4I1,	1	SLC16A3	1.351351351
MATK		COX5A,COX5B,COX6A1,COX6B1,			
		COX7B,COX7C,COX8A,CS,IDH3A,			
		IDH3B,IDH3G,ME2,MPC1,MPC2,			
		NDUFA1,NDUFA11,NDUFA12,			
		NDUFA13,NDUFA2,NDUFA3, NDUFA4,NDUFA6,NDUFA7,NDUFB1,			
		NDUFB10,NDUFB11,NDUFB2,			
		NDUFB4,NDUFB7,NDUFB8,NDUFS7,			
		NDUFS8,NRF1,PDK1,PDK2,PDK3,			
		PDK4,PDP1,PEMT,SLC16A1,			
		SLC16A3,SLC16A8,TFAM,UQCR10, UQCR11,UQCRQ,ATP6V1F,D2HGDH,			
		FAHD1,FH,IDH2,L2HGDH,NCOA2,			
		NCOR1,OGDH,PDHA1,PPARGC1A,			
		SDHB,SDHC,SOD2,GLUD1,PRKAB1,			
		PRKAG1,PRKAA2,PRKAB2,PRKAG2,			
		LDHA,LDHB,LDHC,SDHA			

Table 2

Top Pathways with Downregulated Genes in CCA. This table lists the top enriched pathways associated with downregulated genes in cholangiocarcinoma (CCA). The columns include the pathway name, the total number of genes in the pathway (Total_Gene_Count_in_Pathway), the number of downregulated genes (Dwnr_Gene_Count) and the percentage of downregulated genes within each pathway. Key pathways such as epigenetic regulation, transcriptional regulation, and AMPK signaling show the highest proportion of downregulated genes, indicating their potential role in CCA pathogenesis.

Dwnr_Gene_Count	Dwnr_Genes_Under_Pathway	Percentage
10	CYP4A11,CYP4A22,ACAT1,ADH1A,ADH1B,	41.66667
	ADH1C,ADH4,ADH6,ALDH2,EHHADH	
10	CYP1A1,CYP1A2,KMO,TDO2,AADAT,CAT,	31.25
	ALDH2,ACAT1,AOX1,EHHADH	
22	AADAT,ACAT1,ADH1A,ADH1B,ADH1C,ADH4,	23.15789
	ADH6,AGXT,ALDH2,AMDHD1,AOX1,CPS1,	
	DMGDH,EHHADH,FOLH1,FTCD,GATM,GLS2,	
	GLYAT,HPD,MAT1A,SDS	
9	G6PC,PCK1,PCK2,ADH1A,ADH1B,ADH1C,	22.5
	ADH4,ADH6,ALDH2	
3	OTC,CPS1,GLS2	18.75
5	APOA1,CYP8B1,TTR,AOX1,APOB	17.85714
4	ASPG,FOLH1B,FOLH1,GLS2	11.42857
5	G6PC,GYS2,HNF4A,PCK1,PCK2	10.41667
1	SLC6A12	6.666667
1	RGN	5.263158
4	GYS2,G6PC,PCK1,PCK2	4.819277
1	APOB	3.030303
1	GLS2	2.631579
1	APOB	2.564103
1	CAT	2.325581
1	HNF4A	1.694915
1	AOX1	0.806452

-21.58 kcal/mol, mapped between nucleotides 323-354 of lnc-SLC6A12-7:5 and 979-1010 of SLC6A12, which was optimal for stable binding (Figs. 5b, g & S2c). We further validated the expression of SLC6A12 in the TCGA-CHOL dataset using the UALCAN database (Chandrashekar et al., 2022) and observed its downregulation in 36 patient samples. Additionally, other cancers such as cervical squamous cell carcinoma and endocervical adenocarcinoma, glioblastoma, and lung squamous cell carcinoma also exhibited downregulation of SLC6A12. Survival analysis revealed that by 2000 days post-diagnosis, only 2 out of the 36 patients survived (Fig. S3a-S3b). Additionally, STRING analysis identified interacting partners of the 84 DEMGs, with genes directly linked to SLC6A12 grouped separately. Apart from this, we analysed gene interactions using the 84 DEMGs, focusing on SLC6A12 to identify genes directly associated with its function. To eliminate weak connections and outliers in the network map, we applied MCL clustering and observed that SLC6A12 interacted exclusively with GAD1 in the 12th cluster (Fig. 5c). The immediate interacting partner of interest was GAD1. Hence, IntaRNA analysis of the shortlisted lncRNAs with GAD1 also revealed a strong interaction score. The pair lnc-SLC6A12-1:3 and GAD1 showed an interaction energy of -22.05 kcal/mol, spanning nucleotides 401-547 of lnc-SLC6A12-1:3 and 3005-3150 of GAD1 near the 3' UTR of the transcripts (Figs. 5d, h & S2b). Similarly, the interaction between lnc-SLC6A12-7:5 and GAD1 exhibited an energy of -18.06 kcal/mol, involving nucleotides 183-213 of lnc-SLC6A12-7:5 and 2405-2432 of GAD1, also near the 3' UTR (Figs. 5e, h & S2d). This suggests a stable interaction of these lncRNAs with GAD1. GAD1 was consistently upregulated, whereas lnc-SLC6A12-1:3, lnc-SLC6A12-7:5, and SLC6A12 were downregulated across all analysed samples. This expression pattern was further validated using the TCGA cholangiocarcinoma dataset, which demonstrated the same trend across all 35 tumour samples (Fig. 5f). GAD1 was overexpressed in at least 12 cancers in TCGA and downregulated in 4 cancers and survival analysis showed less than two patients survived after 2000 days of diagnosis (Fig. S4a-b). As part of our validation, we used lncTAR to assess the interactions between the shortlisted lncRNAs and their

target mRNAs. The analysis showed that Inc-SLC6A12-1:3 interacts with both SLC6A12 (dG = -19.02 kcal/mol) and GAD1 (dG = -13.50 kcal/mol). Similarly, Inc-SLC6A12-7:5 was found to interact with SLC6A12 (dG = -11.35 kcal/mol) and GAD1 (dG = -16.51 kcal/mol). These negative dG values suggest that the interactions are thermodynamically favourable and support the regulatory roles proposed for these IncRNAs (Supplementary file 2).

3.5. interaction analysis of lnc-SLC6A12 variants with key enriched transcription factors

The DEMGs were used as input for the CiiiDER tool, with the background set to genes having an l2fc between -0.4 and 0.4. From this analysis, the top 10 enriched transcription factors, (*BATF::JUN*, FOSL1, IRF1, *NR2C2*, NR4A1, *NRL*, *Rxra*, *SIX1*, THAP1, *TWIST1*) were identified, where the transcription factors represented to bind to promoter of *GAD1* and *SLC6A12* were THAP1, FOSL1, NR4A1 and IRF1 (Fig. 6a). These transcription factors were then analysed using catRAPID omics v2.1 for lncRNA-Transcription factor interaction (Fig. 6b). lnc-SLC6A12–7:5 exhibited minimal interaction with these transcription factors (data not included in the paper), suggesting that it is unlikely to bind to any of them.

The interaction between lnc-SLC6A12-1:3 and IRF1 revealed two binding sites on lnc-SLC6A12-1:3. The highest interaction propensity of 14.26 was observed in region 2 (nucleotides 501-552 of Inc-SLC6A12-1:3 and amino acids 226-277 of IRF1). Additionally, in region 1, binding occurred between nucleotides 300–350 of lnc-SLC6A12–1:3, interacting with the same region of IRF1, with an interaction propensity of 12.47 (Fig. 6b-d & Table. S1). The interaction matrix revealed that lnc-SLC6A12-1:3 and NR4A1 exhibited two binding sites on NR4A1, with interaction propensities of 11.82 and 11.39, respectively. Region 1 (highlighted in red on the 3D protein structure) involved interaction between nucleotides 501-552 of lnc-SLC6A12-1:3 and amino acids 323-374 of NR4A1. Region 2 (highlighted in lime green on the 3D protein structure) involved interaction between amino acids 426-477 of NR4A1 (Fig. 6b-d & Table. S1). The interaction matrix showed that Inc-SLC6A12-1:3 interacts with THAP1 between nucleotides 501-552 and amino acids 138-189, with an interaction propensity of 42.94 (Fig. 6b-d & Table. S1). Additionally, lnc-SLC6A12-1:3 demonstrated the highest binding affinity with FOSL1, with a peak interaction propensity of 12.47, occurring between nucleotides 501-552 and amino acids 171-222 (Fig. 6b-d & Table. S1).

4. Discussion

The study utilized a dataset comprising 18 normal liver tissue samples and 16 tumour CCA samples from SRP159264. Its primary aim was to identify novel lncRNAs in cholangiocarcinoma (CCA) patients that regulate the expression of key metabolic genes associated with CCA. The nCounter® Metabolic Pathways Panel was used to annotate 748 metabolic genes in tumour samples. A filtering process, based on a p-value threshold of less than 0.05, identified 494 significantly expressed mRNAs. Further, 41 overexpressed mRNAs with L2FC greater than 2 and 43 downregulated mRNAs with an L2FC less than -2. Next, we analysed the pathways associated with these genes. The upregulated genes were distributed across 22 enriched cellular metabolic pathways (CMPs), while the downregulated genes were associated with 17 depleted CMPs. Eleven pathways exhibited dual regulation, with both upregulated and downregulated genes.

The top enriched CMPs with upregulated genes included autophagy, fatty acid synthesis, and the PI3K pathway, all of which play significant roles in cancer metabolism and have been widely reported in various malignancies. Autophagy, a crucial mechanism for cellular homeostasis, has been implicated in cancer progression by regulating metabolic reprogramming and promoting survival under stress conditions (Pandey et al., 2021; Xie et al., 2020). Additionally, lipid metabolism and

Screening Biologically significant IncRNAs from DEMG-Associated Loci

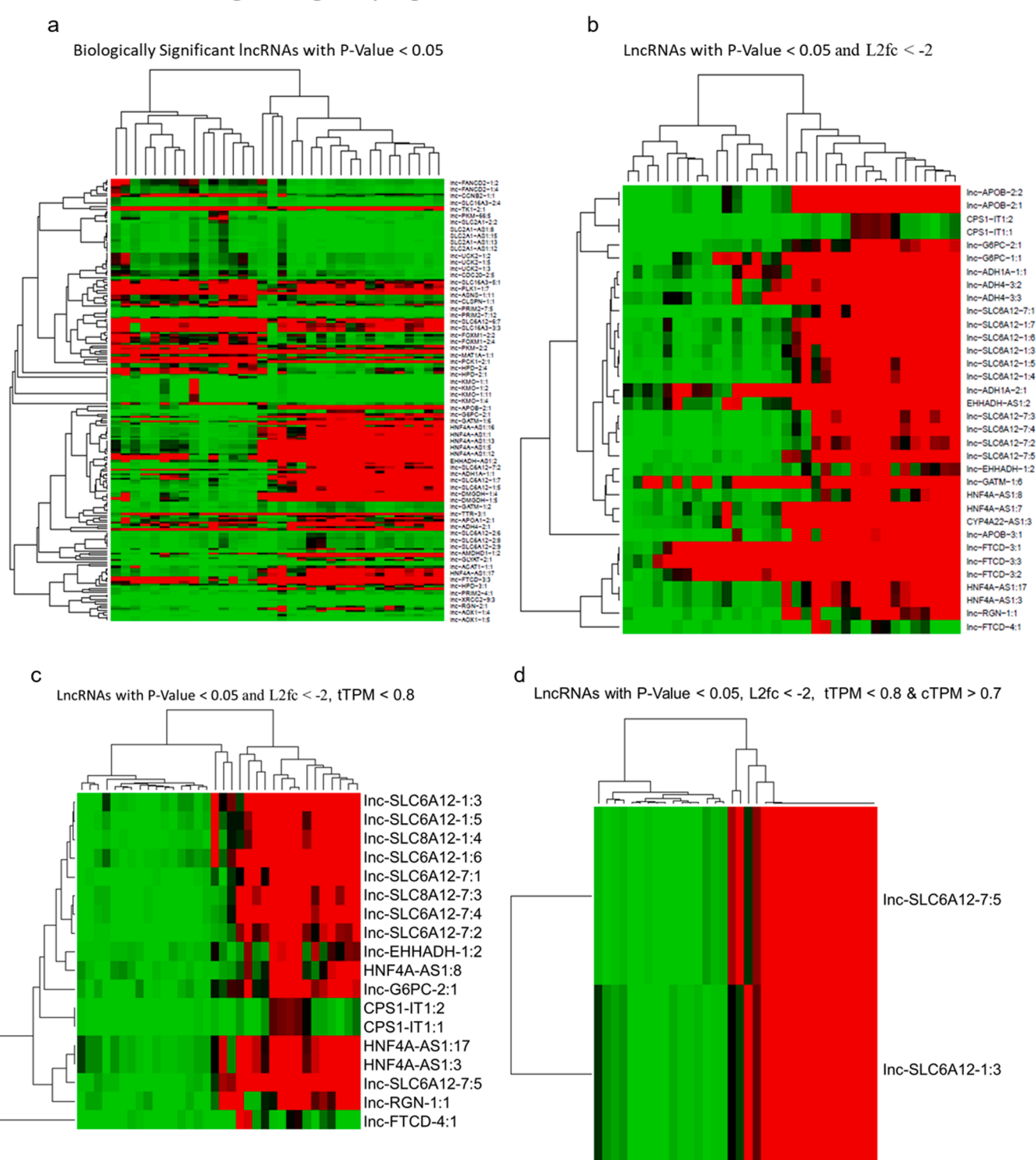
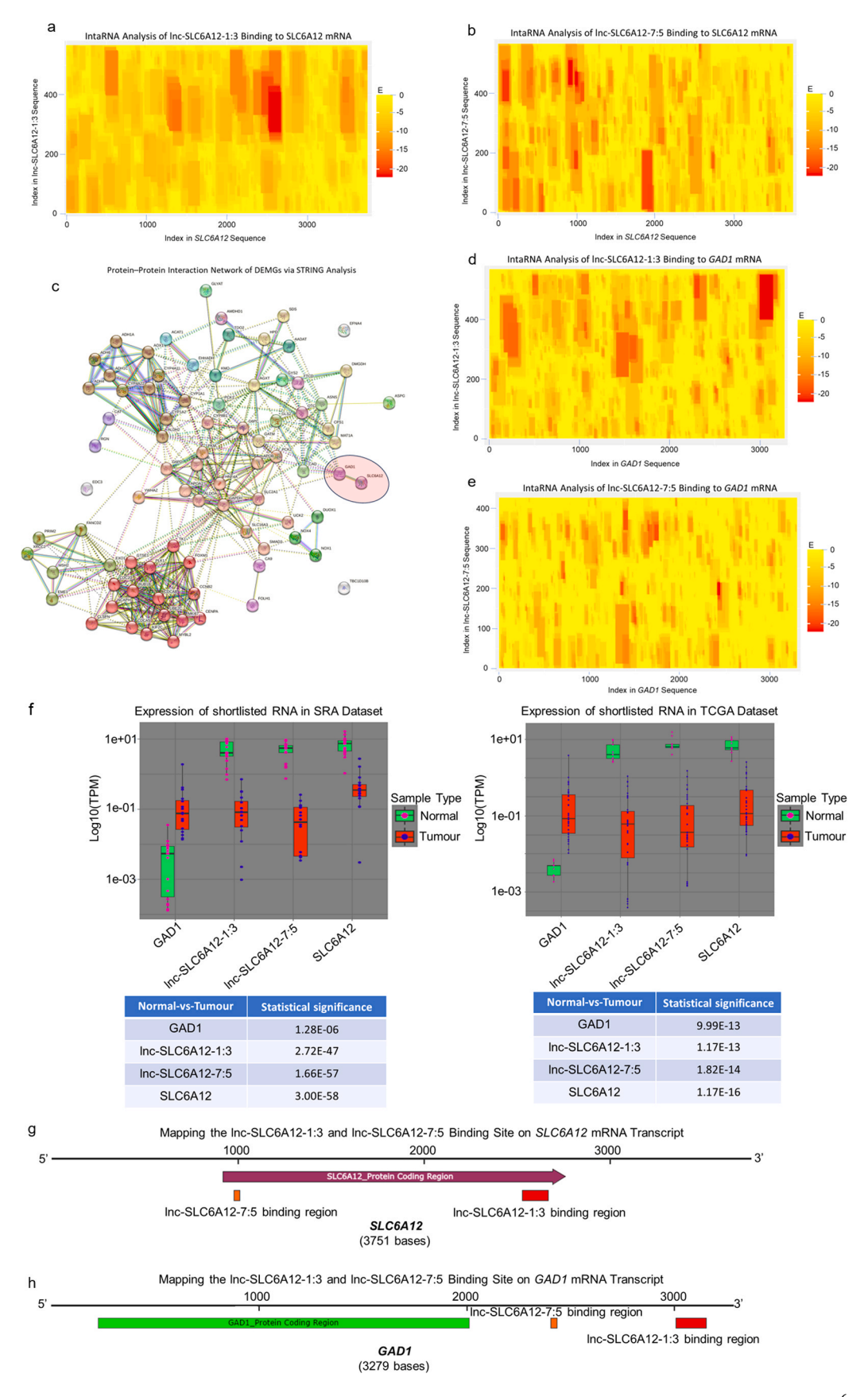


Fig. 4. Analysis of lncRNA expression patterns using TPM normalised data. Heatmap Comparison across the Datasets with Filtering Based on Defined Parameters to Shortlist Upregulated lncRNAs. a. Heatmap showing the expression of lncRNAs with p-value less than 0.05. b. Heatmap showing the expression of lncRNAs, focusing only on those with a p-value less than 0.05 and l2fc less than -2. c. Heatmap presenting the expression of lncRNAs, with p-value less than 0.05, l2fc less than -2 and tumour samples TPM value less than 0.8. d. Heatmap presenting the expression of lncRNAs, with p-value less than 0.05, l2fc less than -2, tumour samples TPM value less than 0.8 and TPM of Normal samples greater than 0.7. (Green denotes low expression and Red denotes high expression).

autophagy are intricately linked, where dysregulated lipid homeostasis contributes to tumour growth and therapy resistance (Alizadeh et al., 2023; Xie et al., 2020). Moreover, the PI3K signalling pathway, a key regulator of cancer metabolism, drives tumourigenesis by modulating

glucose and lipid metabolism, making it a critical therapeutic target (Han et al., 2024). While these pathways haven't been studied in CCA, our current findings independently show their enrichment, further highlighting their importance in CCA progression. The top depleted



(caption on next page)

Fig. 5. Heatmap displaying the Interaction of lncRNA with mRNA across various RNA pairs, highlighting all the possible intermolecular interactions at potential binding sites. a. Heatmap showing all the possible interactions between lnc-SLC6A12–1:3 and SLC6A12, displaying the binding site and associated binding energy. (Yellow denotes low interaction and Red denotes high interaction in Heatmaps showing lncRNA-mRNA interactions) b. Heatmap illustrating all the possible interactions between lnc-SLC6A12–1:3 and SLC6A12, based on binding energy scores. c. STRING analysis depicting direct and functional interactions involving SLC6A12. d. Heatmap showing interaction between lnc-SLC6A12–1:3 and GAD1, showing the binding site and corresponding binding energy. e. Heatmap showing interaction between lnc-SLC6A12–7:5 and GAD1, indicating the binding site and associated binding energy. f. Box and whisker plot showing expression of GAD1, lnc-SLC6A12–1:3, lnc-SLC6A12–7:5 and SLC6A12 (Green box represents normal samples and red box represents Tumour samples) in both SRA and TCGA Datasets. P-values associated with the analysis are presented in the table. g. Schematic representation of the SLC6A12 mRNA and the specific sites where lncRNAs interact with the SLC6A12 mRNA. The purple arrow represents the protein-coding region of the SLC6A12–1:3 interacts. h. Schematic representation of the GAD1 mRNA and the specific sites where lncRNAs interact with the specific sites where lncRNAs interact with the GAD1 mRNA. The lime green arrow represents the protein-coding region of the GAD1 transcript. The orange feature shows the region where lnc-SLC6A12–7:5 binds to GAD1, and the red rectangle marks the region on GAD1 where lnc-SLC6A12–1:3 interacts.

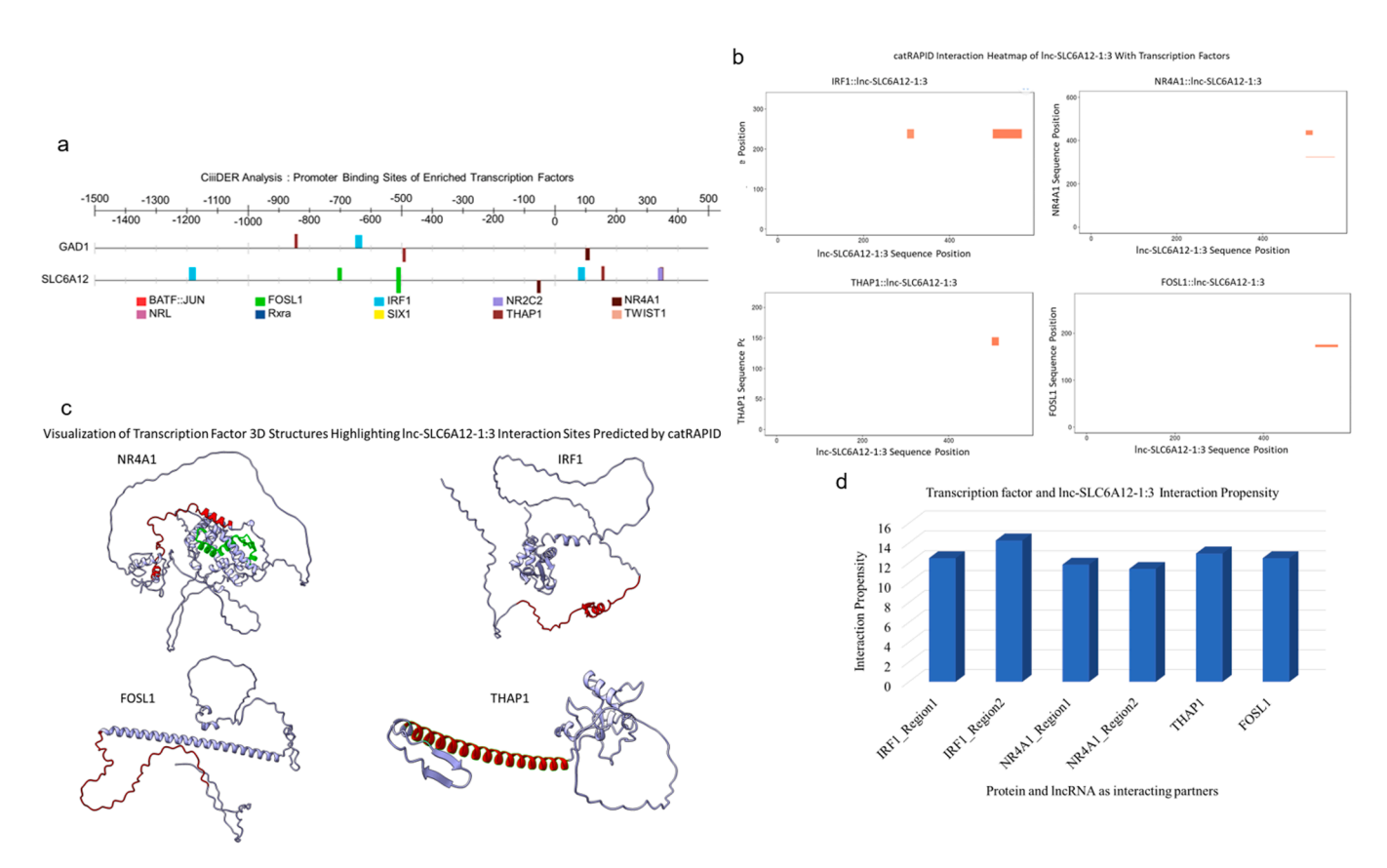


Fig. 6. Interaction of lncRNA with Transcription factors. a. CiiiDER site map showing transcription factors binding sites on *GAD1* and *SLC6A12* promoter. b. catRAPID interaction plot showing the region of interaction between lnc-SLC6A12–1:3 and IFR1, NR4A1, THAP1 and FOSL1 transcription factors respectively. c. 3D protein structure of NR4A1, IFR1, FOSL1 and THAP1 highlighting the region of interaction with the lnc-SLC6A12–1:3. Red denoted Region1 interaction site and Lime Green is the Region2 interaction site, tinted pastel blue represents the region which do not interact with the lncRNA. d. Bar graph showing the interaction propensity of lnc-SLC612–1:3 with IRF1, NR4A1, THAP1 and FOSL1.

pathways associated with the downregulated genes included AMPK, antigen presentation, and glucose transport. Reports suggest that AMPK enhances glucose transport by phosphorylating TXNIP and TBC1D1, promoting plasma membrane localisation of GLUT1 and GLUT2. This increases cellular glucose uptake, utilization, and glycolysis by activating PFKFB3, which regulates the glycolytic rate-limiting enzyme PFK1 (Marsin et al., 2002; Wang et al., 2024). The downregulation of AMPK observed in our study correlates with the suppression of the glucose transport pathway. In response to this metabolic shift, GABA synthesis and the GABA shunt pathway are upregulated through the overexpression of GAD1 in CCA, supporting alternative energy production and tumour survival. Similarly, antigen presentation plays a pivotal role in allowing the immune system to recognize and eliminate malignant cells. However, cancer cells evade immune detection by downregulating antigen presentation to immune cells, a phenomenon known as immune evasion. The suppression of this pathway in CCA may

contribute to its ability to escape immune surveillance, further supporting tumour progression (Kallingal et al., 2023; Marsin et al., 2002). The downregulation of AMPK observed in our study correlates with the suppression of the glucose transport pathway. In response to this metabolic shift, as observed in our study GABA synthesis and the GABA shunt pathway are upregulated through the overexpression of GAD1 in CCA, supporting alternative energy production and tumour survival. Dual regulation was observed in pathways such as PI3K and glutamine metabolism, indicating a complex regulatory effect, which has also been reported in other cancers (The Role of Glutamine Metabolism in Experimental and Human Intrahepatic Cholangiocarcinoma - University of Regensburg Publication Server, n.d.). Reactome and DAVID analysis revealed significant GO terms, such as heme binding and retinol metabolic processes, with pathways related to metabolism, amino acid derivatives, and cell division showing enrichment These observations have already been made in several other cancer studies (Hanahan and

Weinberg, 2011).

lncRNAs overlapping the genomic loci of the shortlisted 84 DEMGs were systematically screened, and only those meeting the following selection criteria were included in the analysis: p-value < 0.05, log2 fold change (L2FC) > 2 or < -2, transcript per million (TPM) values between 0.7 and 0.8 in both normal and tumour samples respectively. Two lncRNAs, lnc-SLC6A12-1:3 and lnc-SLC6A12-7:5, fulfilled these conditions and were selected for further analysis. LncRNAs function by RNA-DNA, RNA-RNA and RNA-protein interactions to regulate various cellular processes. RNA-RNA interactions have been extensively studied in miRNAs (Afonso-Grunz and Müller, 2015). Notably, even small and imperfectly matched regions of nucleotide complementarity can facilitate specific interactions, as evidenced by the strong ability of micro-RNAs to target mRNA using short, imperfect seed sequences selectively (Cisse et al., 2012; Kumari et al., 2023; Roy et al., 2024). lncRNA also has a similar ability to bind to mRNA (Sebastian-Delacruz et al., 2021). We further examined to determine if there is a direct plausible interaction between the lncRNA and mRNA pair using the IntaRNA tool. The results showed the strongest interaction between nucleotides 283-409 of lnc-SLC6A12-1:3 and the 3' end of the CDS of SLC6A12, specifically between nucleotides 2526-2665. On the other hand, lnc-SLC6A12-7:5 displayed a strong interaction with SLC6A12 near 5' end of CDS. The data indicates that suggest that lnc-SLC6A12-7:5 has the potential to bind to the 5' end of SLC6A12, whereas lnc-SLC6A12-1:3 may interact with its 3' end. This differential binding further implies that these lncRNAs could exert distinct regulatory influences on SLC6A12. We analysed the expression of these lncRNAs about their binding sites on mRNA and observed a positive correlation, where both the lncRNAs and SLC6A12 mRNA were downregulated in cancer cells. This suggests that, in normal cells, the binding of these lncRNAs to the mRNA may enhance its stability. To further validate this finding, we analysed the expression of lnc-SLC6A12-1:3 and lnc-SLC6A12-7:5 and SLC6A12 in the TCGA-CHOL dataset and observed its consistent downregulation across all 35 patients, reinforcing its potential significance in cholangiocarcinoma (CCA).

In addition to analysing mRNAs co-localised with lncRNAs at the same genomic loci, we explored whether these lncRNAs could potentially interact with other DEMGs located at distant loci. Using STRING analysis on the 84 DEMGs, we identified GAD1 (GAD67) as a key interacting partner of SLC6A12/BGT1 at the protein level. Interestingly, GAD1 mRNA was found to be significantly overexpressed in our dataset. Given that both SLC6A12/BGT1 and GAD1/GAD67 are linked through the GABAergic pathway, we hypothesised that GAD1 might also interact with lnc-SLC6A12-1:3 and lnc-SLC6A12-7:5, suggesting a possible cross-locus regulatory mechanism mediated by these lncRNAs. Hence, looked for a possible direct interaction between lnc-SLC6A12-1:3, lnc-SLC6A12-7:5 and GAD1; the result showed that both lncRNAs, lnc-SLC6A12-1:3 and lnc-SLC6A12-7:5, had a propensity to bind to the 3'UTR region of GAD1 mRNA. Such lncRNA-mRNA interaction could either trigger degradation of mRNA or increase stability (Gong and Maquat, 2011; Kumari et al., 2023; Mercer and Mattick, 2013; Roy et al., 2024; Sun et al., 2016). A study revealed that FGFR3-AS1 forms a tail-to-tail complementary pairing with FGFR3 mRNA, protecting its 3'UTR from RNase digestion and stabilising FGFR3 mRNA, thereby upregulating its expression. These pairing counters miRNA-mediated degradation of FGFR3 mRNA at its 3'UTR (Sun et al., 2016). Additionally, other evidence also suggests that lncRNAs binding to the 3'UTR can stabilise mRNAs (Zhang, Wen, 2024). Conversely, another study showed that Alu elements within lncRNAs partially pair with the 3' UTR of actively translating mRNAs, forming a double-stranded RNA structure. This structure is then targeted by Staufen1, triggering the degradation of the mRNA (Gong and Maquat, 2011; Mercer and Mattick, 2013). A similar observation was made with miR-501, where overexpression of the pre-miRNA construct led to the production of mature miRNAs, resulting in a corresponding decrease in RAG1 expression through direct binding to its 3'UTR. Whereas, inhibition with anti-miRs increased RAG1

levels (Kumari et al., 2023; Roy et al., 2024). Since this study is purely in silico, experimental validation falls beyond its scope. However, we have inferred the potential mechanisms of action of lnc-SLC6A12-1:3 and lnc-SLC6A12-7:5 through indirect speculation. These findings provide a basis for future experimental studies to further investigate their functional roles. We speculate that lnc-SLC6A12-1:3 and lnc-SLC6A12-7:5 might be involved in triggering the degradation of GAD1 mRNA by binding to the 3'UTR in the nucleus, as the expression of lncRNA and mRNA is negatively correlated. Binding of lncRNA to the 3' UTR of mRNA can also inhibit translation by disrupting the interaction with the 5' cap. This was shown in a study where overexpression of LncRNA 7SL hindered the translation of the tumour suppressor P53. The lncRNA interacted with the 3' UTR of P53's mRNA, preventing HuR from binding and thereby blocking translation (Abdelmohsen et al., 2014; Song et al., 2021). Similarly, lnc-SLC6A12-1:3 and lnc-SLC6A12-7:5 interact with the 3' UTR of GAD1, potentially contributing to translational repression in normal cells. This mechanism may help regulate GABA levels at both transcriptional and translational levels. To further validate this finding, we analysed GAD1 expression in the TCGA-CHOL dataset and found it to be overexpressed in all 36 patients, reinforcing its significance in cholangiocarcinoma (CCA) as highlighted in this study.

In addition to their regulatory roles through mRNA binding, lncRNAs are capable of interacting with proteins such as transcription factors, potentially modulating their activity and function. Hung et al. demonstrated that lncRNA PANDA interacts with NF-YA to suppress apoptosisrelated gene expression, while lncRNA PVT1 inhibits MYC phosphorylation and degradation, whereas rhabdomyosarcoma 2-associated transcripts (RMST) facilitate SOX2 binding to neurogenic transcription factor promoters, acting as its transcriptional coregulator (Hung et al., 2011; Long et al., 2017; Ng et al., 2013; Tseng et al., 2014). Therefore, to investigate whether these lncRNAs can bind to transcription factors and, if so, to understand the mechanism of action through which they exert their effects, we selected the top 10 enriched transcription factors using the CiiiDER tool which revealed that the transcription factors THAP1, NR4A1, and IRF1 play crucial roles in regulating the gene expression of both GAD1 and SLC6A12 by binding to its promoters. Whereas, FOSL1 exclusively binds to the SLC6A12 promoter (Fig. 6a). Using the catRAPID platform, lnc-SLC6A12-1:3 was predicted to strongly interact with the transcription factors THAP1, NR4A1, IRF1, and FOSL1, with several of them targeting overlapping regions, indicating possible competition for binding. Notably, one region of the lncRNA appears to bind both IRF1 and the SLC6A12 mRNA, suggesting a functional overlap. While the lncRNA may still interact with the mRNA through a partially non-overlapping segment, IRF1 seems to require the entire stretch for binding. In contrast, lnc-SLC6A12-7:5 showed minimal or no interaction with the tested transcription factors.

Following the identification of potential lncRNA-transcription factor interactions, we aimed to assess whether the lncRNA binding sites on these transcription factors are accessible for interaction or structurally constrained due to stable secondary structure formation. Additionally, we sought to determine whether such interactions might influence the functional activity of the transcription factors, either by activating or repressing their function based on the binding region on the protein. The lncRNA and transcription factor interaction might lead to two different fates, where lnc-SLC6A12-1:3 may either recruit transcription factors to the promoters of GAD1 and SLC6A12 or inactivate them. To investigate lncRNA-transcription factor (TF) interactions, we analysed their binding at the 3D protein level to determine whether the lncRNA binds within key functional domains of the transcription factors. Binding within a functional domain is likely to disrupt or modify the transcription factor's function. supporting this hypothesis, studies have shown that GAS5 binds to the DNA-binding domain (DBD) of the glucocorticoid receptor (GR) and inhibits GR-induced transcriptional activity (Kino et al., 2010). While binding outside the functional domain may facilitate TF recruitment to target genes. Additionally, if the lncRNA interaction sites for mRNA and TF are distinct, it could act as both a cis and trans regulator

simultaneously, modulating gene expression through multiple mechanisms. The results showed that lnc-SLC6A12-1:3 interacts with the disordered regions of IRF1 and FOSL1 (Fig. 6c), suggesting that lnc-SLC6A12-1:3 binding may play a role in recruiting these transcription factors rather than inhibiting their function. Also, the propensity for interaction with the SLC6A12 promoter is higher than the GAD1 promoter. This is because the SLC6A12 promoter contains two binding sites for each of these transcription factors, whereas the GAD1 promoter has only one IRF1 binding site and no FOSL1 binding site (Fig. 6a). This supports the observation that SLC6A12 mRNA is downregulated when lnc-SLC6A12-1:3 levels are reduced in CCA, indicating a potential regulatory role of the lncRNA in maintaining SLC6A12 expression. Whereas, GAD1 expression requires either of THAP1 or NR4A1 transcription factors binding to its promoter (Fig. 6a), THAP1 has highly conserved zinc finger domain at its N-terminal region facilitating DNA binding, while the coiled-coil domain (amino acids 139-190) is at its C-terminal region (Richter et al., 2017). The catRAPID data suggests that lnc-SLC6A12-1:3 interacts with the C-terminal coiled-coil domain of THAP1 between 138 and 189 amino acids (Fig. 6c). Hence, this interaction may decrease THAP1 activity in normal cells. Whereas in CCA, as the lncRNA is downregulated, the activity of THAP1 is restored, hence the GAD1 is overexpressed. In case of NR4A1 (TR3), lnc-SLC6A12-1:3 interacts with it between amino acids 323-477, a region where four known domains are associated with it, namely RXRa binding domain, NGFI-B response element (NBRE) - containing DNA, the nuclear receptor C4-type (NR C4) and the nuclear receptor ligand-binding domain (NR LBD) (UNIProt_P22736_NR4A1_HUMAN). Www.Uniprot.Org. Retrieved January 30, 2025, from Https://Www.Uniprot.Org/Un iprotkb/P22736/Entry#family_and_domains, n.d.; Zhao et al., 2007). This interaction suggests that lnc-SLC6A12-1:3 binding shows decreased activity of NR4A1 due to the masking of all the above four domains in a normal cell. Whereas in CCA, as the lnc-SLC6A12-1:3 is downregulated, the activity of NR4A1 is restored, hence the GAD1 is overexpressed, which is similar to the interaction with lncRNA and THAP1. Using integrative analyses from CiiiDER (for promoter TF enrichment), catRAPID (for lncRNA-protein interaction predictions), and Protein3D structural modelling, we reveal that lnc-SLC6A12-1:3 and lnc-SLC6A12-7:5 regulate the balance of SLC6A12 and GAD1 expression by binding to key transcription factors (IRF1, FOSL1, THAP1, NR4A1), where they promote SLC6A12 expression by recruiting activating TFs to its promoter and suppress GAD1 expression by inhibiting repressive TF activity, thereby maintaining normal GABA metabolism—a balance that is lost when these lncRNAs are downregulated in cancer.

A key strength of this study is its integrative approach, combining differential expression analysis with interaction prediction to identify novel lncRNAs linked to cholangiocarcinoma. By focusing on those associated with metabolic genes, we explore an underexamined aspect of CCA—metabolic reprogramming. The predicted lncRNA-mRNA and lncRNA-transcription factor interactions offer mechanistic insights and provide a strong foundation for future functional validation. While this study is based on in silico analysis of bulk RNA-seq data, we addressed this limitation by using strict expression criteria and high-stringency filters to reduce false positives. The selected lncRNAs and their interacting mRNAs showed consistent expression patterns across all CCA patients, adding confidence to our findings. Still, experimental validation through single-cell and functional studies will be important to confirm their roles.

In summary, based on these results, we speculate that in normal cells, lnc-SLC6A12–1:3 and lnc-SLC6A12–7:5 regulate the expression of *SLC6A12* and *GAD1* through multiple interactions. Lnc-*SLC6A12*-1:3 binds to *SLC6A12* in cis and *GAD1* in trans while also interacting with transcription factors IRF1, THAP1, NR4A1 and FOSL1, with IRF1 having the highest binding affinity. Lnc-*SLC6A12*-1:3 recruits IRF1 and FOSL1 to the promoter of *SLC6A12*, enhancing its expression, while binding to THAP1 and NR4A1 reduces their activity, keeping *GAD1* levels in check.

Additionally, lnc-SLC6A12–1:3 binds to the 3' CDS and lnc-SLC6A12–7:5 to the 5' CDS of *SLC6A12*, potentially increasing mRNA stability (indicated by green circles). Conversely, their binding to the 3' UTR of *GAD1* decreases its stability (purple circles) (Fig. 7). This regulation ensures that *SLC6A12* expression remains slightly higher and *GAD1* expression lower in normal cells, maintaining lower GABA levels. *SLC6A12/BGT1* imports extracellular GABA, to prevent silencing of the immune system and thus prevent tumour microenvironment formation. In cancer cells, both lnc-SLC6A12–1:3 and lnc-SLC6A12–7:5 are downregulated. This leads to unchecked *GAD1/GAD67* expression and elevated GABA synthesis, meeting the high energy demands of cancer cells. At the same time, reduced *SLC6A12* levels decrease GABA import, fostering the tumour microenvironment. This shift highlights the contrasting roles of these lncRNAs in normal and cancer cell GABA metabolism and their impact on tumour progression (Fig. 7).

5. Conclusion

A major strength of this study lies in the novel identification of two previously uncharacterized long non-coding RNAs, lnc-SLC6A12–1:3 and lnc-SLC6A12–7:5, as potential upstream regulators of GAD1 and SLC6A12, respectively. These findings suggest a role for these lncRNAs in modulating the GABAergic pathway to meet the elevated energy demands observed in cholangiocarcinoma (CCA). While these insights are based on robust computational analyses, future experimental validation is crucial to confirm these predicted lncRNA–mRNA interactions.

Therapeutic targeting of SLC6A12 may be challenging, as it plays a complex role in cancer metabolism regardless of its expression levels. When overexpressed, SLC6A12 facilitates GABA import into tumour cells, fueling the GABA shunt to meet energy needs. Conversely, when downregulated, extracellular GABA accumulates and may aid tumour progression through microenvironmental modulation—though direct evidence in CCA remains limited.

In contrast, GAD1 presents a more compelling therapeutic target. Its inhibition can directly block intracellular GABA synthesis, disrupting the GABA shunt and impairing energy supply to tumour cells. Moreover, reduced GABA levels in the tumour microenvironment could diminish invasion, migration, and immune evasion. GAD1 has also been implicated as a hub gene associated with drug resistance, clinicopathological features, and immune microenvironment in prostate cancer (Wan et al., 2023)While L-Allylglycine is known to inhibit GAD after biotransformation into 2-keto-4-pentenoic acid via stereospecific amino acid oxidase (Abshire et al., 1988). Its clinical use is limited by safety concerns, including seizure induction in animal models (Thomas and Yang, 1991). Hence, there is a need for safer, specific *GAD1* inhibitors.

Restoration of *Inc-SLC6A12–1:3* and *Inc-SLC6A12–7:5* expression represents an innovative therapeutic strategy. Technologies such as CRISPR activation (CRISPRa) can selectively enhance their transcription, while synthetic lncRNA mimics could be employed to rescue their function. These approaches offer promising avenues to re-establish the regulatory roles of these lncRNAs and counteract their dysregulation in CCA.

Overall, this study contributes new insights into the regulatory landscape of the GABAergic pathway in cholangiocarcinoma, identifying *lnc-SLC6A12–1:3*, *lnc-SLC6A12–7:5*, and *GAD1* as promising candidates for future therapeutic development.

CRediT authorship contribution statement

SMA and NSD contributed equally to the study design, data collection, analysis, and interpretation. SMA prepared the initial draft of the manuscript, and NSD provided critical revisions and final approval. Both authors have read and approved the final manuscript and agree to be accountable for all aspects of the work.

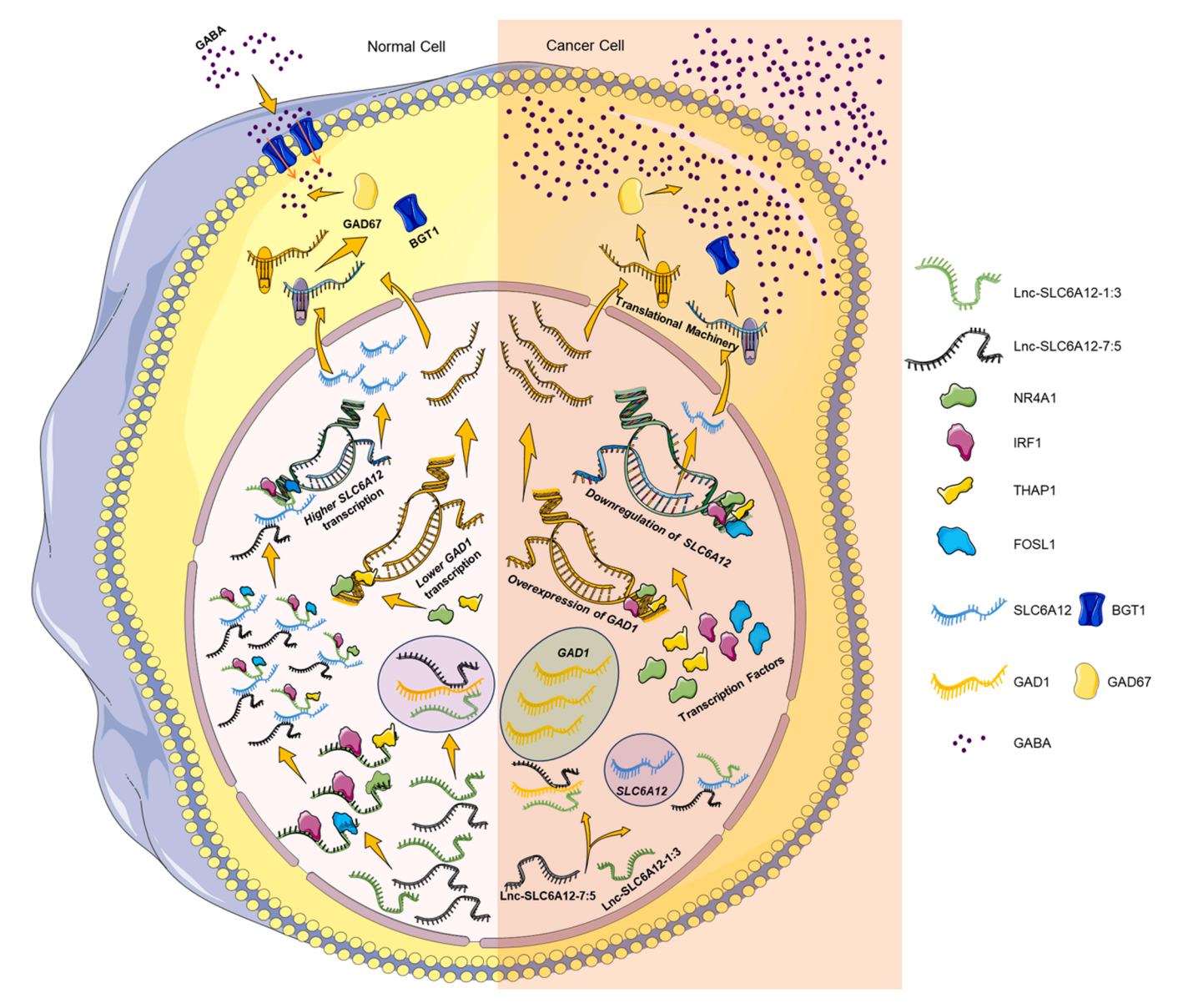


Fig. 7. The illustration depicts the regulatory roles of lnc-SLC6A12–1:3 and lnc-SLC6A12–7:5 in modulating *SLC6A12* and *GAD1* expression in normal and cancer cells. In normal cells, lnc-SLC6A12–1:3 recruits transcription factors (IRF1 and FOSL1) to the promoter of *SLC6A12*, enhancing its expression, while binding to THAP1 and NR4A1 reduces their activity, keeping *GAD1* levels low. The binding of lnc-SLC6A12–1:3 and lnc-SLC6A12–7:5 to specific mRNA regions increases *SLC6A12* stability (indicated by green circles) and decreases *GAD1* stability (purple circles). This regulation maintains low GABA synthesis while allowing GABA import via *SLC6A12*, preventing tumour microenvironment formation. In cancer cells, the downregulation of both lncRNAs disrupts this balance, resulting in increased *GAD1* expression and elevated GABA synthesis to meet tumour energy demands. Concurrently, reduced *SLC6A12* levels limit GABA import, promoting tumour microenvironment development. These findings highlight the contrasting regulatory roles of lnc-SLC6A12–1:3 and lnc-SLC6A12–7:5 in normal and cancer cells.

Funding

The project did not receive any specific funding. SMA was supported by a Senior Research Fellowship (SRF) from the Council of Scientific and Industrial Research (CSIR), Government of India.

Declaration of Generative AI and AI-assisted technologies in the writing process

We utilised ChatGPT to rephrase sentences in this work to enhance clarity and conciseness. After generating rephrased content, we carefully reviewed and edited it as necessary, ensuring accuracy and taking full responsibility for the final published article.

Declaration of Competing Interest

The authors declare that they have no known competing financial interests or personal relationships that could have appeared to influence the work reported in this paper.

Acknowledgments

SMA is supported by Senior Research Fellowship (SRF) from the Council of Scientific and Industrial Research (CSIR), Government of India, and gratefully acknowledges the same. We appreciate the support of Prof. Sathees C. Raghavan (Department of Biochemistry, Indian Institute of Science, Bangalore), Dr. Sagar Desai, and Prof. Bibha Choudhary (Institute of Bioinformatics and Applied Biotechnology,

Bangalore). We also thank Dr. Nitu Kumari (Department of Cell and Developmental Biology, Northwestern University, USA) for proof-reading the manuscript. We thank The Cancer Genome Atlas (TCGA) for providing access to the TCGA-CHOL controlled dataset used in this study.

Appendix A. Supporting information

Supplementary data associated with this article can be found in the online version at doi:10.1016/j.compbiolchem.2025.108562.

References

- Abdelmohsen, K., Panda, A.C., Kang, M.J., Guo, R., Kim, J., Grammatikakis, I., Yoon, J. H., Dudekula, D.B., Noh, J.H., Yang, X., Martindale, J.L., Gorospe, M., 2014. 7SL RNA represses p53 translation by competing with HuR. Nucleic Acids Res. 42 (15), 10099–10111. https://doi.org/10.1093/NAR/GKU686.
- Abshire, V.M., Hankins, K.D., Roehr, K.E., DiMicco, J.A., 1988. Injection of L-allylglycine into the posterior hypothalamus in rats causes decreases in local GABA which correlate with increases in heart rate. Neuropharmacology 27 (11), 1171–1177. https://doi.org/10.1016/0028-3908(88)90013-5.
- Afonso-Grunz, F., Müller, S., 2015. Principles of miRNA-mRNA interactions: Beyond sequence complementarity. Cell. Mol. Life Sci. 72 (16), 3127–3141. https://doi.org/10.1007/S00018-015-1922-2/METRICS.
- Alizadeh, J., Kavoosi, M., Singh, N., Lorzadeh, S., Ravandi, A., Kidane, B., Ahmed, N., Mraiche, F., Mowat, M.R., Ghavami, S., 2023. Regulation of autophagy via carbohydrate and lipid metabolism in cancer. Cancers 15 (8), 2195. https://doi.org/ 10.3390/CANCERS15082195.
- Andrews S. (2010). FastQC: a quality control tool for high throughput sequence data. \(\lambda \text{ttp://www.bioinformatics.babraham.ac.uk/projects/fastqc}\).
- Armaos, A., Colantoni, A., Proietti, G., Rupert, J., Tartaglia, G.G., 2021. catRAPID omics v2.0: going deeper and wider in the prediction of protein–RNA interactions. Nucleic Acids Res. 49 (W1), W72–W79. https://doi.org/10.1093/NAR/GKAB393.
- Balázs, R., Machiyama, Y., Hammond, B.J., Julian, T., Richter, D., 1970. The operation of the γ-aminobutyrate bypath of the tricarboxylic acid cycle in brain tissue in vitro. Biochem. J. 116 (3), 445. https://doi.org/10.1042/BJ1160445.
- Banales, J.M., Marin, J.J.G., Lamarca, A., Rodrigues, P.M., Khan, S.A., Roberts, L.R., Cardinale, V., Carpino, G., Andersen, J.B., Braconi, C., Calvisi, D.F., Perugorria, M.J., Fabris, L., Boulter, L., Macias, R.I.R., Gaudio, E., Alvaro, D., Gradilone, S.A., Strazzabosco, M., Gores, G.J., 2020. Cholangiocarcinoma 2020: the next horizon in mechanisms and management. 2020 17:9 Nat. Rev. Gastroenterol. Hepatol. 17 (9), 557–588. https://doi.org/10.1038/s41575-020-0310-z.
- Bhatt, M., Gauthier-Manuel, L., Lazzarin, E., Zerlotti, R., Ziegler, C., Bazzone, A., Stockner, T., Bossi, E., 2023. A comparative review on the well-studied GAT1 and the understudied BGT-1 in the brain. Front. Physiol. 14, 1145973. https://doi.org/ 10.3389/FPHYS.2023.1145973/BIBTEX.
- Cao, J., Chen, X., Lu, G., Wang, H., Zhang, X., Yang, H., & Bai, Y. (2021). Identification of Prognostic Gene Signature Associated with Tumour Microenvironment of Cholangiocarcinoma. https://doi.org/10.21203/RS.3.RS-524410/V1.
- Chandrashekar, D.S., Karthikeyan, S.K., Korla, P.K., Patel, H., Shovon, A.R., Athar, M., Netto, G.J., Qin, Z.S., Kumar, S., Manne, U., Crieghton, C.J., Varambally, S., 2022. UALCAN: an update to the integrated cancer data analysis platform. Neoplasia (N. Y. N. Y.) 25, 18–27. https://doi.org/10.1016/J.NEO.2022.01.001.
- Cisse, I.I., Kim, H., Ha, T., 2012. A rule of seven in Watson-Crick base-pairing of mismatched sequences. 2012 19:6 Nat. Struct. Mol. Biol. 19 (6), 623–627. https:// doi.org/10.1038/nsmb.2294.
- Dennis, G., Sherman, B.T., Hosack, D.A., Yang, J., Gao, W., Lane, H.C., Lempicki, R.A., 2003. DAVID: database for annotation, visualization, and integrated discovery. Genome Biol. 4 (9), 1–11. https://doi.org/10.1186/GB-2003-4-9-R60/TABLES/3.
- Desai, S.S., Whadgar, S., Raghavan, S.C., Choudhary, B., 2022. MiRAGDB: a knowledgebase of RAG regulators. Front. Immunol. 13, 863110. https://doi.org/ 10.3389/FIMMU.2022.863110/BIBTEX.
- Elgenidy, A., Afifi, A.M., Jalal, P.K., 2022. Survival and causes of death among patients with intrahepatic cholangiocarcinoma in the United States from 2000 to 2018. Cancer Epidemiol. Biomark. Prev. 31 (12), 2169–2176. https://doi.org/10.1158/ 1055-9965.EPI-22-0444/709188/AM/SURVIVAL-AND-CAUSES-OF-DEATH-AMONG-PATIENTS-WITH.
- Franceschini, A., Szklarczyk, D., Frankild, S., Kuhn, M., Simonovic, M., Roth, A., Lin, J., Minguez, P., Bork, P., Von Mering, C., Jensen, L.J., 2013. STRING v9.1: proteinprotein interaction networks, with increased coverage and integration. Nucleic Acids Res. 41 (D1). D808–D815. https://doi.org/10.1093/NAR/GKS1094.
- Gearing, L.J., Cumming, H.E., Chapman, R., Finkel, A.M., Woodhouse, I.B., Luu, K., Gould, J.A., Forster, S.C., Hertzog, P.J., 2019. CiiiDER: A tool for predicting and analysing transcription factor binding sites. PLOS ONE 14 (9), e0215495. https:// doi.org/10.1371/JOURNAL.PONE.0215495.
- Genus, T., Tataru, D., Morement, H., Toledano, M., Khan, S., 2019. late submission poster) Incidence and mortality rates of cholangiocarcinoma in England. Ann. Oncol. 30, iv155. https://doi.org/10.1093/annonc/mdz183.007.
- Gil, N., Ulitsky, I., 2019. Regulation of gene expression by cis-acting long non-coding RNAs. 2019 21:2 Nat. Rev. Genet. 21 (2), 102–117. https://doi.org/10.1038/ s41576-019-0184-5.

- Gong, C., Maquat, L.E., 2011. lncRNAs transactivate Staufen1-mediated mRNA decay by duplexing with 3'UTRs via Alu elements. Nature 470 (7333), 284. https://doi.org/ 10.1038/NATURF09701.
- Han, B., Lin, X., Hu, H., 2024. Regulation of PI3K signaling in cancer metabolism and PI3K-targeting therapy. Transl. Breast Cancer Res. 5, 33. https://doi.org/10.21037/ TBCR-24-29.
- Hanahan, D., Weinberg, R.A., 2011. Hallmarks of cancer: the next generation. Cell 144 (5), 646–674. https://doi.org/10.1016/J.CELL.2011.02.013/ASSET/2067D218-2368-451A-B4DA-CF9EF4807B23/MAIN.ASSETS/GR1.JPG.
- Huang, D., Alexander, P.B., Li, Q.J., Wang, X.F., 2022. GABAergic signaling beyond synapses - an emerging target for cancer therapy. Trends Cell Biol. 33 (5), 403. https://doi.org/10.1016/J.TCB.2022.08.004.
- Hung, T., Wang, Y., Lin, M.F., Koegel, A.K., Kotake, Y., Grant, G.D., Horlings, H.M., Shah, N., Umbricht, C., Wang, P., Wang, Y., Kong, B., Langerød, A., Børresen-Dale, A. L., Kim, S.K., Van De Vijver, M., Sukumar, S., Whitfield, M.L., Kellis, M., Chang, H.Y., 2011. Extensive and coordinated transcription of noncoding RNAs within cell-cycle promoters. 2011 43:7 Nat. Genet. 43 (7), 621–629. https://doi.org/10.1038/ng.848.
- Kallingal, A., Olszewski, M., Maciejewska, N., Brankiewicz, W., Baginski, M., 2023. Cancer immune escape: the role of antigen presentation machinery. J. Cancer Res. Clin. Oncol. 149 (10), 8131. https://doi.org/10.1007/S00432-023-04737-8.
- Karolchik, D., Hinricks, A.S., Furey, T.S., Roskin, K.M., Sugnet, C.W., Haussler, D., Kent, W.J., 2004. The UCSC Table browser data retrieval tool. Nucleic Acids Res. 32 (Database). https://doi.org/10.1093/NAR/GKH103.
- Katz, K., Shutov, O., Lapoint, R., Kimelman, M., Rodney Brister, J., O'Sullivan, C., 2022. The sequence read archive: a decade more of explosive growth. Nucleic Acids Res. 50 (D1), D387–D390. https://doi.org/10.1093/NAR/GKAB1053.
- Kempson, S.A., Zhou, Y., Danbolt, N.C., 2014. The betaine/GABA transporter and betaine: roles in brain, kidney, and liver. Front. Physiol. 5, 81573. https://doi.org/ 10.3389/FPHYS.2014.00159/BIBTEX.
- Kino, T., Hurt, D.E., Ichijo, T., Nader, N., Chrousos, G.P., 2010. Noncoding RNA Gas5 Is a growth arrest and starvation-associated repressor of the glucocorticoid receptor. Sci. Signal. 3 (107), ra8. https://doi.org/10.1126/SCISIGNAL.2000568.
- Kleinrok, Z., Matuszek, M., J. J.-J. of physiology, & 1998. (1998). GABA content and GAD activity in colon tumours taken from patients with colon cancer or from xenografted human colon cancer cells growing as sc tumours in athymic. Agro.Icm. Edu.PIZ Kleinrok, M Matuszek, J Jesipowicz, B Matuszek, A Opolski, C RadzikowskiJournal of Physiology and Pharmacology, 1998•agro.Icm.Edu.Pl. (https://agro.icm.edu.pl/agro/element/bwmeta1.element.agro-article-260ed672-1090-4c 91-bfbd-1676ee6eaef7).
- Kumari, R., Roy, U., Desai, S., Nilavar, N.M., Van Nieuwenhuijze, A., Paranjape, A., Radha, G., Bawa, P., Srivastava, M., Nambiar, M., Balaji, K.N., Liston, A., Choudhary, B., Raghavan, S.C., 2021. MicroRNA miR-29c regulates RAG1 expression and modulates V(D)J recombination during B cell development. Cell Rep. 36 (2). https://doi.org/10.1016/J.CELREP.2021.109390/ATTACHMENT/D35A465D-B99C-40E8-8817-93FB38A183D5/MMC2.PDF.
- Kumari, R., Roy, U., Desai, S., Mondal, A.S., Nair, R.R., Nilavar, N., Choudhary, B., Raghavan, S.C., 2023. MicroRNA, miR-501 regulate the V(D)J recombination in B cells. Biochem. J. 480 (24), 2061–2077. https://doi.org/10.1042/BCJ20230250.
- cells. Biochem. J. 480 (24), 2061–2077. https://doi.org/10.1042/BCJ20230250.
 Lange, M.D., Jüngling, K., Paulukat, L., Vieler, M., Gaburro, S., Sosulina, L., Blaesse, P., Sreepathi, H.K., Ferraguti, F., Pape, H.C., 2014. Glutamic acid decarboxylase 65: a link between GABAergic synaptic plasticity in the lateral amygdala and conditioned fear generalization. 2014 39:9 Neuropsychopharmacology 39 (9), 2211–2220. https://doi.org/10.1038/npp.2014.72.
- Li, T.J., Jiang, J., Tang, Y.L., Liang, X.H., 2023. Insights into the leveraging of GABAergic signaling in cancer therapy. Cancer Med. 12 (13), 14498. https://doi.org/10.1002/CAM4.6102.
- Long, Y., Wang, X., Youmans, D.T., Cech, T.R., 2017. How do lncRNAs regulate transcription? Sci. Adv. 3 (9), eaao2110. https://doi.org/10.1126/SCIADV. AAO2110.
- Louis, C., Papoutsoglou, P., Coulouarn, C., 2020. Molecular classification of cholangiocarcinoma. Curr. Opin. Gastroenterol. 36 (2), 57–62. https://doi.org/ 10.1097/MOG.0000000000000011.
- Love, M.I., Huber, W., Anders, S., 2014. Moderated estimation of fold change and dispersion for RNA-seq data with DESeq2. Genome Biol. 15 (12), 1–21. https://doi. org/10.1186/S13059-014-0550-8/FIGURES/9.
- Mann, M., Wright, P.R., Backofen, R., 2017. IntaRNA 2.0: enhanced and customizable prediction of RNA–RNA interactions. Nucleic Acids Res. 45 (WebServer), W435. https://doi.org/10.1093/NAR/GKX279.
- Marsin, A.S., Bouzin, C., Bertrand, L., Hue, L., 2002. The stimulation of glycolysis by hypoxia in activated monocytes is mediated by AMP-activated protein kinase and inducible 6-phosphofructo-2-kinase. J. Biol. Chem. 277 (34), 30778–30783. https:// doi.org/10.1074/jbc.M205213200.
- Matuszek, M., Jesipowicz, M., monitor, science, Z.K.-M., 2001. GABA content and GAD activity in gastric cancer. & 2001 Europepmc.OrgM Matuszek, M Jesipowicz, Z KleinrokMedical Science Monitor: International Medical Journal of Experimental, 2001•europepmc.Org. (https://europepmc.org/article/med/11386012).
- Mazurkiewicz, M., Opolski, A., J. W.-... of experimental, 1999. GABA level and GAD activity in human and mouse normal and neoplastic mammary gland. &, & 1999 Europepmc. OrgM Mazurkiewicz A Opolski J Wietrzyk C Radzikowski Z KleinrokJournal Experimental Clinical Cancer Research CR 1999•europepmc. Org. (https://europepmc.org/article/med/10464715).
- Mercer, T.R., Mattick, J.S., 2013. Structure and function of long noncoding RNAs in epigenetic regulation. 2013 20:3 Nat. Struct. Mol. Biol. 20 (3), 300–307. https://doi. org/10.1038/nsmb.2480
- Milacic, M., Beavers, D., Conley, P., Gong, C., Gillespie, M., Griss, J., Haw, R., Jassal, B., Matthews, L., May, B., Petryszak, R., Ragueneau, E., Rothfels, K., Sevilla, C.,

- Shamovsky, V., Stephan, R., Tiwari, K., Varusai, T., Weiser, J., D'Eustachio, P., 2024. The reactome pathway knowledgebase 2024. Nucleic Acids Res. 52 (D1), D672–D678. https://doi.org/10.1093/NAR/GKAD1025.
- Ng, S.Y., Bogu, G.K., Soh, B.S., Stanton, L.W., 2013. The long noncoding RNA RMST interacts with SOX2 to regulate neurogenesis. Mol. Cell 51 (3), 349–359. https://doi.org/10.1016/j.molcel.2013.07.017.
- Pandey, A., Yadav, P., Shukla, S., 2021. Unfolding the role of autophagy in the cancer metabolism. Biochem. Biophys. Rep. 28, 101158. https://doi.org/10.1016/J. BRRFE 2021 101158
- Patel, T., 2002. Worldwide trends in mortality from biliary tract malignancies. BMC Cancer 2, 10. https://doi.org/10.1186/1471-2407-2-10.
- Quinlan, A.R., Hall, I.M., 2010. BEDTools: a flexible suite of utilities for comparing genomic features. Bioinforma. Appl. NOTE 26 (6), 841–842. https://doi.org/ 10.1093/bioinformatics/btq033.
- Richter, A., Hollstein, R., Hebert, E., Vulinovic, F., Eckhold, J., Osmanovic, A., Depping, R., Kaiser, F.J., Lohmann, K., 2017. In-depth characterization of the homodimerization domain of the transcription factor thap1 and dystonia-causing mutations therein. Journal Molecular Neuroscience MN 62 (1), 11–16. https://doi. org/10.1007/S12031-017-0904-2.
- Roy, U., Desai, S.S., Kumari, S., Bushra, T., Choudhary, B., Raghavan, S.C., 2024. Understanding the role of miR-29a in the regulation of RAGI, a gene associated with the development of the immune system. J. Immunol. 213 (8), 1125–1138. https://doi.org/10.4049/JIMMUNOL.2300344.
- Samborska, B., Griss, T., Ma, E.H., Jones, N., Williams, K.S., Sergushichev, A., Johnson, R.M., Esaulova, E., Loginicheva, E., Flynn, B., Blagih, J., Artyomov, M.N., Jones, R.G., Vincent, E.E., 2021. A non-canonical role for glutamate decarboxylase 1 in cancer cell amino acid homeostasis, independent of the GABA shunt. Short title Regulation cancer cell metabolism GAD 1. https://doi.org/10.1101/2021.02.17.431489.
- Sarasa, S.B., Mahendran, R., Muthusamy, G., Thankappan, B., Selta, D.R.F., Angayarkanni, J., 2020. A brief review on the non-protein amino acid, gammaamino butyric acid (GABA): its production and role in microbes. Curr. Microbiol. 77 (4), 534–544. https://doi.org/10.1007/S00284-019-01839-W/METRICS.
- Sebastian-Delacruz, M., Gonzalez-Moro, I., Olazagoitia-Garmendia, A., Castellanos-Rubio, A., Santin, I., 2021. The role of lncRNAs in gene expression regulation through mRNA stabilization, 2021, Vol. 7, 3 NonCoding RNA 7 (1), 3. https://doi.org/10.3390/NCRNA7010003.
- Song, P., Yang, F., Jin, H., Wang, X., 2021. The regulation of protein translation and its implications for cancer. 2021 6:1 Signal Transduct. Target. Ther. 6 (1), 1–9. https://doi.org/10.1038/s41392-020-00444-9.
- Statistics About Bile Duct Cancer | Cholangiocarcinoma Stats | American Cancer Society. (n. d.). (https://www.cancer.org/cancer/types/bile-duct-cancer/about/key-statistics.html).
- Struys, E.A., Jansen, E.E.W., Gibson, K.M., Jakobs, C., 2005. Determination of the GABA analogue succinic semialdehyde in urine and cerebrospinal fluid by dinitrophenylhydrazine derivatization and liquid chromatography–tandem mass spectrometry: application to SSADH deficiency. J. Inherit. Metab. Dis. 28 (6), 913–920. https://doi.org/10.1007/S10545-005-0111-0
- Sulpice, L., Desille, M., Turlin, B., Fautrel, A., Boudjema, K., Clément, B., Coulouarn, C., 2016. Gene expression profiling of the tumour microenvironment in human intrahepatic cholangiocarcinoma. Genom. Data 7, 229–232. https://doi.org/ 10.1016/J.GDATA.2016.01.012.

- Sulpice, L., Rayar, M., Desille, M., Turlin, B., Fautrel, A., Boucher, E., Llamas-Gutierrez, F., Meunier, B., Boudjema, K., Clément, B., Coulouarn, C., 2013.
 Molecular profiling of stroma identifies osteopontin as an independent predictor of poor prognosis in intrahepatic cholangiocarcinoma. Hepatology 58 (6), 1992–2000. https://doi.org/10.1002/HEP.26577.
- Sun, J., Wang, X., Fu, C., Wang, X., Zou, J., Hua, H., Bi, Z., 2016. Long noncoding RNA FGFR3-AS1 promotes osteosarcoma growth through regulating its natural antisense transcript FGFR3. Mol. Biol. Rep. 43 (5), 427–436. https://doi.org/10.1007/ S11033-016-3975-1/METRICS.
- The Role of Glutamine Metabolism in Experimental and Human Intrahepatic Cholangiocarcinoma University of Regensburg Publication Server. (n.d.). Retrieved January 11, 2025, doi: 10.5283/epub.58648 from https://epub.uni-regensburg.de/58648/
- Thomas, J., Yang, Y.C., 1991. Allylglycine-induced seizures in male and female rats. Physiol. Behav. 49 (6), 1181–1183. https://doi.org/10.1016/0031-9384(91)90348-
- Tseng, Y.Y., Moriarity, B.S., Gong, W., Akiyama, R., Tiwari, A., Kawakami, H., Ronning, P., Reuland, B., Guenther, K., Beadnell, T.C., Essig, J., Otto, G.M., O'Sullivan, M.G., Largaespada, D.A., Schwertfeger, K.L., Marahrens, Y., Kawakami, Y., Bagchi, A., 2014. PVT1 dependence in cancer with MYC copy-number increase. 2014 512:7512 Nature 512 (7512), 82–86. https://doi.org/10.1038/nature13311.
- UNIProt P22736_NR4A1_HUMAN. www.uniprot.org. Retrieved January 30, 2025, from (https://www.uniprot.org/uniprotkb/P22736/entry#family_and_domains). (n.d.).
- Vélez-Fort, M., Audinat, E., & Angulo, M.C. (2011). Central Role of GABA in Neuron–Glia Interactions. (Http://Dx.Doi.Org/10.1177/1073858411403317), 18(3), 237–250. https://doi.org/10.1177/1073858411403317.
- Volders, P.J., Helsens, K., Wang, X., Menten, B., Martens, L., Gevaert, K., Vandesompele, J., Mestdagh, P., 2013. LNCipedia: a database for annotated human lncRNA transcript sequences and structures. Nucleic Acids Res. 41 (D1), D246–D251. https://doi.org/10.1093/NAR/GKS915.
- Wan, L., Liu, Y., Liu, R., Mao, W., 2023. GAD1 contributes to the progression and drug resistance in castration resistant prostate cancer. Cancer Cell Int. 23 (1), 1–15. https://doi.org/10.1186/S12935-023-03093-4/FIGURES/7.
- Wang, N., Wang, B., Maswikiti, E.P., Yu, Y., Song, K., Ma, C., Han, X., Ma, H., Deng, X., Yu, R., Chen, H., 2024. AMPK-a key factor in crosstalk between tumour cell energy metabolism and immune microenvironment? 2024 10:1 Cell Death Discov. 10 (1), 1–13. https://doi.org/10.1038/s41420-024-02011-5.
- Xie, Y., Li, J., Kang, R., Tang, D., 2020. Interplay between lipid metabolism and autophagy. Front. Cell Dev. Biol. 8, 431. https://doi.org/10.3389/ FCFIJ.2020.00431.
- Young, S.Z., Bordey, A., 2009. GABA's control of stem and cancer cell proliferation in adult neural and peripheral niches. Physiology 24 (3), 171. https://doi.org/10.1152/PHYSIOL.00002.2009.
- Zhang Nianjie, & Wen Kunming. (2024). The role of lncRNA binding to RNA-binding proteins to regulate mRNA stability in cancer progression and drug resistance mechanisms. (https://www.spandidos-publications.com/10.3892/or.2024.8801).
- Zhao, W.X., Tian, M., Zhao, B.X., Li, G.D., Liu, B., Zhan, Y.Y., Chen, H.Z., Wu, Q., 2007. Orphan receptor TR3 attenuates the p300-induced acetylation of retinoid X receptoralpha. Mol. Endocrinol. 21 (12), 2877–2889. https://doi.org/10.1210/ME.2007-0107